Subsolidus and Partial Melting Reactions in the Quartz-excess $CaO+MgO+Al_2O_3+SiO_2+H_2O$ System under Water-excess and Water-deficient Conditions to 10 kb: Some Implications for the Origin of Peraluminous Melts from Mafic Rocks

by DAVID JOHN ELLIS[1]* AND ALAN BRUCE THOMPSON[2]

[1]*Department of Geology, University of Tasmania, Hobart, Tasmania, Australia*
[2]*Department fur Erdwissenschaften, ETH-Zentrum, Ch-8092 Zurich, Switzerland*

(*Received 4 November 1984; revised typescript accepted 12 May 1985*)

ABSTRACT

Experimental results up to 10 kb pressure are presented on the stability of amphibole in the quartz-excess $CaO+MgO+Al_2O_3+SiO_2+H_2O$ (CMASH) system under H_2O-excess and H_2O-deficient conditions. Amphibole is stable above the solidus under H_2O-excess conditions whereas under H_2O-deficient conditions dehydration melting of amphibole-bearing assemblages defines the solidus. The successive appearance of amphibole, talc, and zoisite with increasing pressure considerably modifies the plagioclase-pyroxene-garnet-kyanite reactions documented experimentally in the $CaO+MgO+Al_2O_3+SiO_2$ system for gabbro-granulite-eclogite transitions. Although both clinopyroxene and cordierite (with anorthite + orthopyroxene + quartz) may melt eutectically at one atmosphere to form diopside-normative and corundum-normative melts respectively, at higher pressures under H_2O-excess conditions the peritectic melting of mafic rock compositions produces corundum-normative liquids together with either clinopyroxene or amphibole. Dehydration melting produces melts which are not corundum-normative. These data are used to discuss the origins and evolution of contrasting basalt-andesite-dacite-rhyolite volcanic suites and granitic plutons, many of whose silicic variants are corundum-normative in character, such as the Toba Tuff ignimbrites, Indonesia (Beddoe-Stephens *et al.*, 1983) and I-type granite minimum melts (White & Chappell, 1977). In contrast, it is proposed that for the Cascades basalt-andesite-dacite-rhyolite suite the orthopyroxene-plagioclase-quartz thermal divide was maintained up to rhyolite compositions, thereby prohibiting the derivation of corundum-normative rocks from diopside-normative parent magmas.

The deduced reaction relations between pyroxenes, amphibole, plagioclase, quartz, and liquid are used to explain the absence or extreme scarcity of hydrous phases in some hydrous magmas. These phase relations can also explain the development of later plagioclase overgrowths on resorbed plagioclase cores in granitic intrusives, and the general absence of resorption and overgrowths in chemically equivalent extrusive rocks.

A theoretical analysis of the partial melting of forsterite-bearing assemblages in the $CaO+MgO+Al_2O_3+SiO_2+H_2O$ system shows that under H_2O-excess conditions partial melting may generate corundum-normative (but low SiO_2) melts from a peridotite source at shallow depths.

1. INTRODUCTION

Mineral reactions in quartz-bearing mafic rocks have been used to divide the granulite facies into low, medium and high pressure terrains (Green & Ringwood, 1967). Experimental

* Present address: Department of Geology, Australian National University, PO Box 4, Canberra, ACT 2601, Australia.

investigations of natural rock compositions (e.g. Green & Ringwood, 1967) and simple systems (e.g. Kushiro & Yoder, 1966; Hensen, 1976; Hansen, 1981) have documented the low pressure reaction of plagioclase + orthopyroxene to garnet + clinopyroxene + quartz and the higher pressure reaction of garnet + plagioclase to clinopyroxene + kyanite. Although these reactions are univariant in the $CaO + MgO + Al_2O_3 + SiO_2$ (CMAS) system they are continuous (sliding) reactions in natural rocks because of solid solution in feldspar, pyroxenes, and garnet (Green & Ringwood, 1967).

Model amphibolite–granulite transitions in the presence of H_2O have received less attention experimentally than these anhydrous reactions (see Essene *et al.*, 1970). An important result of the addition of H_2O to the $CaO + MgO + Al_2O_3 + SiO_2$ system is to stabilize hydrates at low temperatures and considerably lower the solidus temperature. Both have the effect of replacing the anhydrous granulite reactions by a large number of amphibolite dehydration and melting reactions, which form the basis of this study.

Metamorphosed mafic rocks are likely to constitute a large volume of the lower continental and oceanic crusts as amphibolites. Their predominant mineralogy in the amphibolite facies is hornblende and plagioclase with varying amounts of quartz, chlorite, epidote, talc or orthopyroxene, garnet, low-Ca amphiboles, clinopyroxene, biotite with minor amounts of Fe–Ti oxides and Fe-sulphides, depending upon the compositions of the basaltic protoliths. Although prograde reactions removing chlorite and garnet frequently consume quartz, many metabasaltic compositions will contain quartz into the melting range. In this context we are particularly concerned as to the nature of liquids produced by melting of hornblende + plagioclase + quartz plus the appropriate accessory minerals listed above or their equivalent higher pressure assemblages, under water-saturated and -deficient conditions.

In her melting experiments on several basaltic compositions at 5 kb P_{H_2O}, Helz (1976) obtained peraluminous liquids coexisting with amphibole + plagioclase or amphibole + clinopyroxene from about 700 °C to 1000 °C. Peraluminous liquids have been observed by several workers in their studies of water-saturated synthetic or natural basaltic compositions over a wide range of P–T conditions. Because in the model basalt systems $CaO + MgO + Al_2O_3 + SiO_2$ (CMAS) and $Na_2O + MgO + Al_2O_3 + SiO_2$ (NMAS) at one atmosphere, the assemblage plagioclase + orthopyroxene + tridymite has been considered to act as a thermal divide (Chinner & Schairer (1962); the quartz-norite divide of O'Hara, 1968 separating a diopside eutectic from a cordierite eutectic), the generation of peraluminous liquids from melting of basaltic compositions in nature must be influenced by pressure and/or the presence of H_2O.

Cawthorn & Brown (1976) proposed that the derivation of Cor-normative melts from a basic parent magma is due to fractionation of amphibole (Dio-normative). However, this can only occur if the apparent quartz-norite divide is broken or crossed by a peritectic reaction; otherwise successive melts will decrease in normative diopside but be prevented from becoming Cor-normative. In this paper it is shown that the apparent quartz–norite thermal divide is broken by a peritectic melting reaction involving either clinopyroxene or amphibole.

Experiments in the model system $CaO + MgO + Al_2O_3 + SiO_2 + H_2O$ (CMASH) were undertaken in the present study, in the vicinity of the quartz- and water-saturated solidus, to model the evolution of anatectic melts produced from amphibolites in the continental and oceanic crusts. Experiments were also carried out on the dehydration melting (V-absent) of amphibole-bearing assemblages in CMASH as well as one atmosphere melting experiments in CMAS. The stability of amphibole as well as the partial melting of peridotite assemblages at water saturation are also discussed. A list of abbreviations is presented in Table 1 and some

TABLE 1

List of abbreviations

Amp	amphibole	Kya	kyanite
Anr	anorthite	L	liquid (silicate melt)
Cor	Corundum	Mul	mullite
Cats	Ca-Tschermaks molecule $CaAl_2SiO_6$	Opx	orthopyroxene
Chl	chlorite	Pyr	pyrope
Cp	corundophyllite	Qtz	quartz
Cl	clinochlore	Sap	sapphirine
Cpx	clinopyroxene	Sil	sillimanite
Crd	cordierite	Spn	spinel
Dio	diopside	Tal	talc
Ens	enstatite	Tr	tremolite $Ca_2Mg_5Si_8O_{22}(OH)_2$
For	forsterite	Tt	$Ca_2Mg_4Al_2Si_7O_{22}(OH)_2$
Gar	garnet	Ts	tschermakite $Ca_2Mg_3Al_4Si_6O_{22}(OH)_2$
Gro	grossular	Trd	tridymite
Ca_2Mg-Gar	$Ca_2MgAl_2Si_3O_{12}$	V	vapour (close to H_2O)
$CaMg_2Gar$	$CaMg_2Al_2Si_3O_{12}$	Wol	wollastonite
H-Crd	hydrous cordierite	Zoi	zoisite

TABLE 2

Some reactions discussed in this paper

Amp + Qtz = Anr + Cpx + Opx + V	(1)	Anr + Tal + Crd + Qtz + V = L	(20)
Amp = Anr + For + Cpx + Opx + V	(2)	Zoi + Amp + Qtz + V = Cpx + L	(21)
Amp = Anr + Cpx + Opx + Qtz + V	(3)	Zoi + Tal + Qtz + V = Amp + L	(22)
Amp + For = Anr + Cpx + Opx + V	(4)	Zoi + Tal + Kya + Qtz + V = L	(23)
Anr + Opx + Qtz + V = Amp + L	(5)	Anr + Tal + Kya + Qtz + V = L	(24)
Anr + Amp + Qtz + V = Cpx + L	(6)	Anr + Tal + Qtz + V = Zoi + L	(25)
Amp + Qtz + V = Cpx + Opx + L	(7)	Anr + Amp + Qtz + V = Zoi + L	(26)
Amp + V = Anr + Cpx + Opx + L	(8)	Anr + Tal + Qtz + V = Amp + L	(27)
Amp = Anr + Opx + Cpx + Qtz + L	(9)	Anr + Crd + Qtz + V = Ky + L	(28)
Anr + Opx + Qtz + V = L	(10)	Tal = Ens + Qtz + V	(29)
Anr + Opx + Cpx + Qtz + V = L	(11)	Zoi + Qtz = Anr + Gro + V	(30)
Anr + Opx + Qtz + V = Cpx + L	(12)	Tal + Kya + Qtz = H-Crd	(31)
Anr + Opx + Crd + Qtz + V = L	(13)	Anr = Dio + $Al_2Mg_{-1}Si_{-1}$ + SiO_2	(32)
Anr + Qtz + V = L	(14)	Anr + Cpx + Opx + H_2O = For + L	(33)
Anr + Amp + Opx + Qtz + V = L	(15)	Anr + Opx + H_2O = Cpx + For + L	(34)
Tal + Crd = Opx + Qtz + V	(16)	Opx + Spn + H_2O = Cpx + For + L	(35)
Zoi + Amp + Qtz = Anr + Cpx + V	(17)	Opx + Cpx + Spn + H_2O = For + L	(36)
Zoi + Tal + Qtz = Anr + Amp + V	(18)	Zoi + Tal + Qtz = Anr + Amp + L	(37)
Zoi + Kya + Qtz = Anr + V	(19)	Zoi + Amp + Qtz = Anr + Cpx + L	(38)

Amp = Tt-Ts for (1) and (2), for all other reactions Amp = Tr-Tt in composition.

reactions discussed here are presented in Table 2. This numbering of reactions is used in subsequent figures.

2. PREVIOUS EXPERIMENTS IN CMASH AS A MODEL FOR AMPHIBOLITE MELTING AND DEHYDRATION

It may be anticipated that phase relations in the quartz and H_2O excess part of the CMASH system reflect aspects of the limiting system reactions in Fig. 1; in particular, that the water-saturated melting in CMASH should be close to that deduced by Stewart (1967) and Boettcher (1970) in CASH, and that the aluminous amphibole stability should be relatable to tremolite stability in CMSH (Boyd, 1959). It was thus expected that in CMASH the amphibole-out curve with or without excess H_2O should overlap the water-saturated solidus

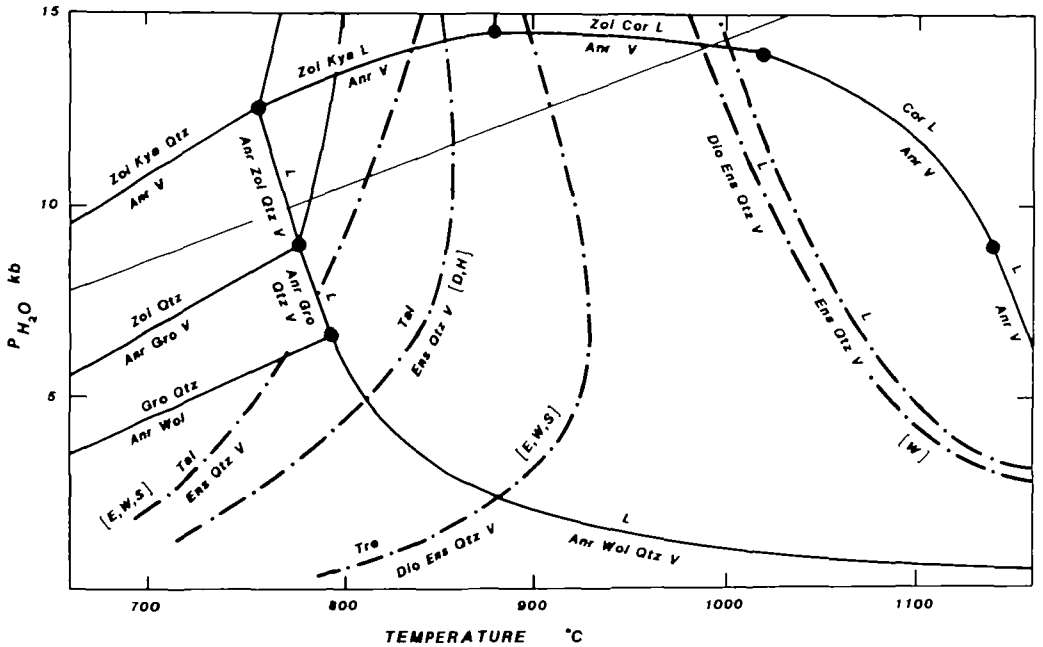

FIG. 1. P–T diagram showing the subsolidus and melting reactions in CASH (solid lines) deduced from experiments by Boettcher (1970, fig. 4) at water-saturation. The dot-dash lines show some equilibria in CMSH: the calculated dehydration reactions of talc and tremolite (Essene *et al.*, 1973; Delaney & Helgeson, 1978) are extrapolated from lower pressure experimental results and labelled [E, W, S] or [D, H] according to which paper they are taken from. The pyroxene–quartz–H_2O eutectics are from Warner (1975).

in the manner discussed by several workers for complex and natural systems (see the summary by Helz, 1982, fig. 52).

In terms of the chosen components the phases anorthite (Anr), zoisite (Zoi), cordierite (Crd), talc (Tal) and quartz (Qtz) may be regarded as pure phases, whereas the amphiboles (Amp) and pyroxenes (Opx and Cpx) exhibit $Al_2Mg_{-1}Si_{-1}$ (TS) and some $CaMg_{-1}$ (CM) exchange. The ideal and observed phase compositions are shown in the ACM (Al_2O_3 + CaO + MgO) projection from SiO_2 and H_2O in Fig. 2A. The $Al_2Mg_{-1}Si_{-1}$ exchange is greater in Amp than Opx and Cpx and consequently the amphibole compositions extend from tremolite (Tr: $Ca_2Mg_5Si_8O_{22}(OH)_2$) to near the $Al_2Mg_{-1}Si_{-1}$ (TS) exchanged composition (Tt: $Ca_2(Mg_4Al)(Si_7Al)O_{22}(OH)_2$).

The low pressure study of synthetic compositions from tremolite (Tr: $Ca_2Mg_5Si_8O_{22}(OH)_2$) to tschermakite (Ts: $Ca_2(Mg_3Al_2)(Si_6Al_2)O_{22}(OH)_2$) by Jasmund & Schäfer (1972) reflects the results of decreasing silica content in the amphiboles through the substitution $Al_2Mg_{-1}Si_{-1}$(TS). They concluded (1972, fig. 1) that the amphibole solutions extended past Tr to $Tr_{45}Ts_{55}$ in the range of 1 to 3 kb P_{H_2O}.

As illustrated in Fig. 2B in a molar $CaMgSi_2O_6$ and H_2O projection on to $CaAl_2SiO_6$ (Cats) + Mg_2SiO_4 (For) + SiO_2 (Qtz); Tr (= + 2 Dio + 3 Ens + 1 Qtz + 1 H_2O) lies on the base between $MgSiO_3$ (Ens) and SiO_2 (Qtz) and towards + $CaMgSi_2O_6$ (Dio); the intermediate amphibole (Tt: $Ca_2(Mg_4Al)(Si_7Al)O_{22}(OH)_2$) lies within the plane of silica-saturation in the hydrous simplified basalt system (at Anr + 3 Ens + Dio + H_2O) and Ts lies at 2 Anr + For + Ens + H_2O at zero Dio. The solid solution in tremolite–tschermakite moves this phase from a quartz-bearing to an olivine-bearing subsolidus topology, effectively piercing the plane Anr + Opx + Cpx in the CMAS system.

One consequence of increasing $Al_2Mg_{-1}Si_{-1}$ in these amphiboles lies with the status of SiO_2 (or Mg_2SiO_4 in appropriate reactions) as a reactant or product of amphibole breakdown. For amphiboles more aluminous than Tt (for example $Tr_{45}Ts_{55}$), the two low-pressure univariant breakdown reactions would be written as:

$$\text{Amp} + \text{Qtz} = \text{Anr} + \text{Cpx} + \text{Opx} + H_2O \quad (1)$$

and

$$\text{Amp} = \text{Anr} + \text{For} + \text{Opx} + \text{Cpx} + H_2O \quad (2)$$

at low pressures. Amphiboles less aluminous than Tt, as observed in our experiments (Table 3), would require that the reactions be written as:

$$\text{Amp} = \text{Anr} + \text{Opx} + \text{Cpx} + \text{Qtz} + H_2O \quad (3)$$

and

$$\text{Amp} + \text{For} = \text{Anr} + \text{Opx} + \text{Cpx} + H_2O. \quad (4)$$

3. EXPERIMENTAL METHODS

Experiments were carried out on a series of glasses, glasses plus synthetic minerals, and mineral mixes with varying compositions in the CMASH. All starting compositions had excess quartz in the subsolidus region (Table 3). These positions with respect to minerals of interest on an ACM diagram are shown in Fig. 2A. Unlike previous studies in this system in which a specific bulk composition was used, our aim was to document the P–T stabilities of specific mineral assemblages. The $CaMg_{-1}$ and $Al_2Mg_{-1}Si_{-1}$ substitutions in some phases necessitated the use of a large number of starting compositions as any one composition was not adequate for crystallizing critical mineral assemblages over a broad P–T interval.

TABLE 3

Starting mix compositions

Mix	*E*	*1*	*2*	*3*	*4*	*5*	*6*	*7*
				Weight per cent oxides				
SiO_2	44·65	47 61	60·15	57·13	55·99	73·41	74·62	74·62
Al_2O_3	23·85	21·60	17·17	11·64	11·41	14·75	15·19	15·19
MgO	14·48	13·20	10·43	18·41	18·04	3·72	6·01	6·01
CaO	17·04	17 57	12·27	12·81	12·55	8·12	4·18	4·18
H_2O					2·00			
				Molar				
A	26·1	24·9	26·1	14·3	14·3	37·9	40·0	40·0
C	33·9	36·7	33·9	28·6	28·6	37·9	20·0	20·0
M	40·0	38·4	40·0	57·1	57·1	24·2	40·0	40·0

Mix E: Glass prepared by melting oxides on Ir strip heater.
Mix 1: Glass E + (Anr + Dio + Zoi + Qtz) mineral mix
Mix 2: Glass E + 28 wt. per cent Qtz.
Mix 3: CMAS oxides (= Tt + Qtz).
Mix 4: Synthesis of Amp + Qtz using Mix 3. Run T-1396.
Mix 5: Anr + Ens + Qtz mineral mix.
Mix 6: Anr + Ens + Crd + Qtz mineral mix.
Mix 7: Glass formed by melting Mix 6.

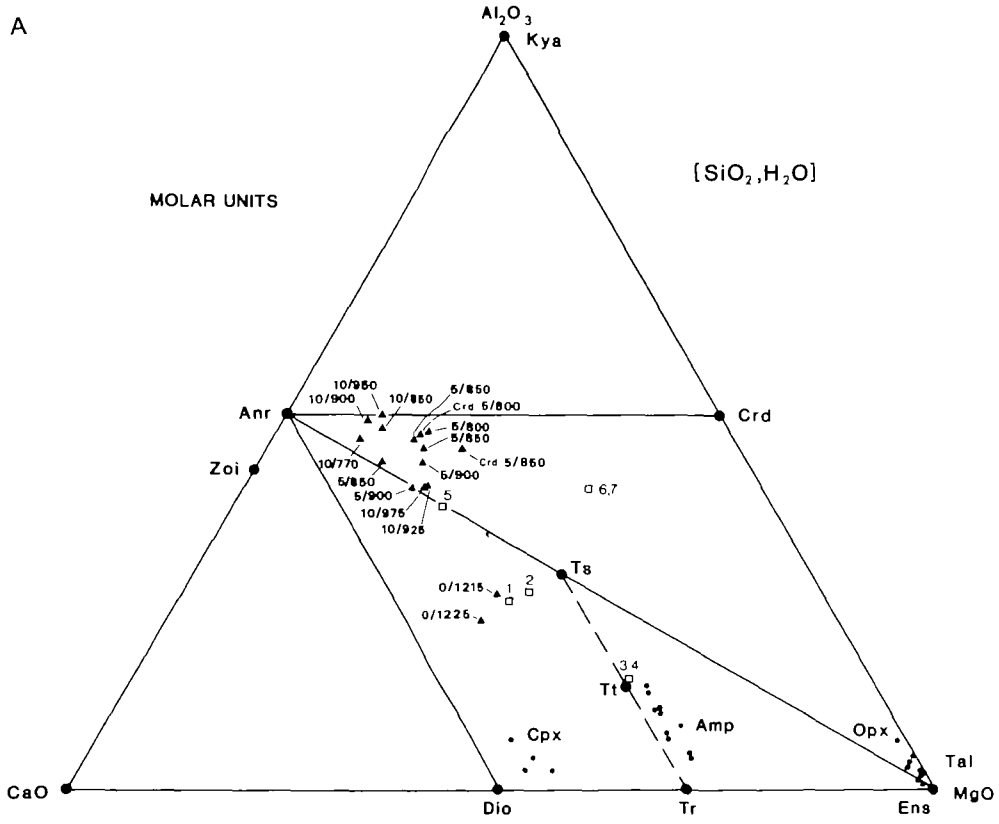

FIG. 2. A. An ACM molar projection from SiO_2 and H_2O on to $Al_2O_3 + CaO + MgO$ showing the composition of pure mineral components (large dots). The range in mineral (small dots) and melt (solid triangles labelled with P(kb)/T °C) compositions synthesized in this study are also shown. Squares numbered 1, 2, etc. refer to starting compositions listed in Table 3 Melts formed from starting compositions 6 and 7 are additionally labelled with Crd. B. (*opposite*) A molar CMS projection from $CaMgSi_2O_6$ and H_2O on to the plane $Mg_2SiO_4 + SiO_2 + CaAl_2SiO_6$ showing the composition of phases projecting below this plane marked negative (−), above the plane as positive (+), and in the plane with a zero (0). The lines of tschermak solid solutions ($Al_2Mg_{-1}Si_{-1}$) are radial to $CaAl_2SiO_6$ in this projection. The planes of silica saturation (Anr + Ens) and silica undersaturation (Anr + For) are shown in projection together with starting mix compositions (1, 2, etc. denoted by open squares) and run product melt compositions (solid triangles).

Synthetic glasses were prepared by thoroughly mixing AR grade oxides (Al_2O_3, SiO_2) and carbonates ($CaCO_3$, $MgCO_3$) together and then melting them to crystal-free glasses using an iridium strip heater (Nicholls, 1974). Molten glasses were homogenized by stirring with a Pt rod and then quenched in a jet of air. These glasses were then ground to < 10 μm size in a agate mortar to enhance chemical homogeneity of each 10 mg aliquot used in the experiments. Three or four large glass fragments were analysed with an electron microprobe to check the starting compositions (Table 3).

Anorthite, zoisite, enstatite, diopside, tremolite, and talc were synthesized from AR grade oxides (Table 4). Orthorhombic zoisite was the stable polymorph found in our experiments, consistent with the recent experimental studies by Jenkins *et al.* (1983) on the relative stabilities of zoisite and clinozoisite.

Tremolite of composition $Ca_2Mg_5Si_8O_{22}(OH)_2$ could not be synthesized, but is always subcalcic ($\sim Ca_{1.9}Mg_{5.1}Si_8O_{22}(OH)_2$) as evidenced by the presence of diopside as a

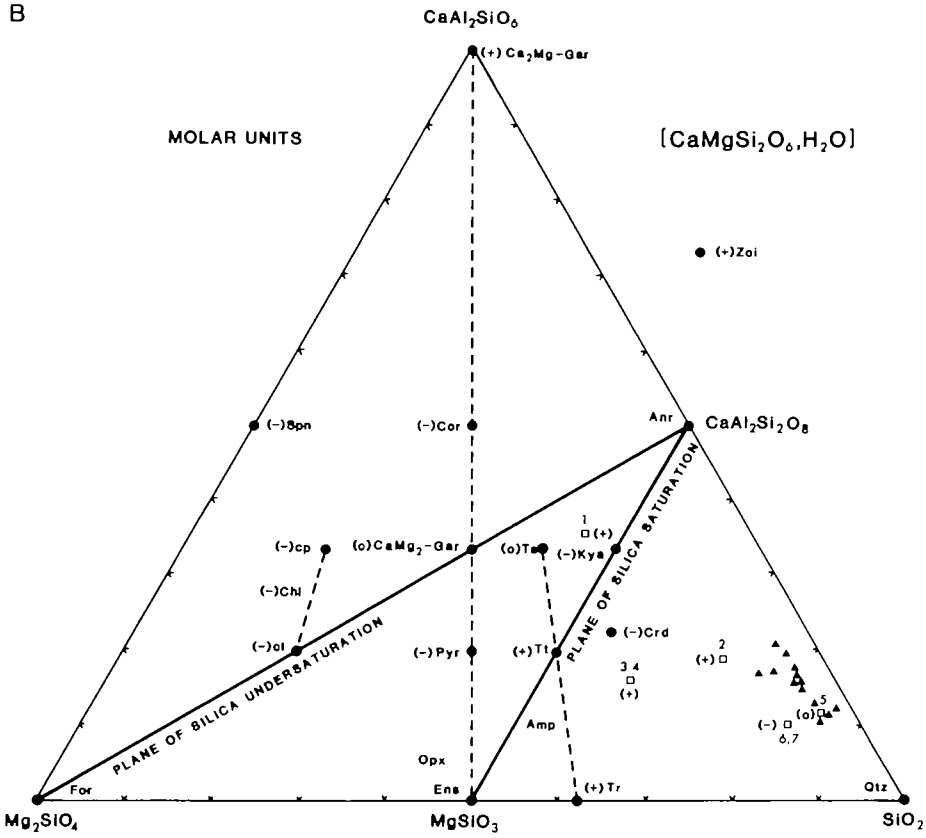

synthesis run product and confirmed by microprobe analysis. This problem has previously been noted (Boyd, 1959; Troll & Gilbert, 1972; Wones & Dodge, 1977). Chatterjee (pers. comm., 1971 to Wones & Dodge, 1977) made a rigorous study of this problem and concluded that tremolite synthesized at 750 °C contains 5 to 10 molecular per cent $Mg_7Si_8O_{22}(OH)_2$.

High pressure experiments were carried out using piston cylinder apparatuses at Zurich and Hobart. Pressure assemblies were similar in both laboratories. Experiments using talc as a pressure medium had a -10 per cent friction correction applied (see Green & Ringwood, 1967, p. 771). A piston-in technique was used. Experimental techniques are similar to those described by Green & Ringwood (1967). Temperature was measured using a $Pt/Pt_{90}Rh_{10}$ thermocouple and temperature was controlled automatically to within ± 5 °C.

Each experiment had 10 mg of starting material together with up to 3 mg of water sealed inside Pt, $Ag_{75}Pd_{25}$, or $Ag_{50}Pd_{50}$ capsules. Capsule weights were noted before and after each experiment in order to determine if H_2O had escaped. Excess water was determined on the basis of a fluid phase bubbling out of the capsule on piercing. Water-excess experiments which did not meet these criteria were not used in the interpretation of H_2O-excess results. Primary vapour was identified in polished mounts by large vesicles in glass. Such bubbles are orders of magnitude larger than the micron-sized vapour bubbles exsolved from glass on quench.

Run products were examined optically using immersion of oil grain mounts and X-ray diffraction. Polished fragments were analysed using the energy dispersive SEM-microprobe at the University of Tasmania. Full correction procedures were employed (Griffin, 1979).

TABLE 4

Run products

Run	*P (kb)*	*T (°C)*	*Time (hours)*	*Starting mix*	*Wt. per cent H_2O*	*Run product*
Z-2	20	900	17	Zoi oxides	15	Zoi
Z-7	10	900	23	Anr oxides	20	Anr
Z-8	10	900	114	CMS oxides	20	Cpx Opx Qtz V
Z-10	30	1100	1	Dio oxides	0	Dio
Z-25	10	800	164	1	25	Amp Anr Qtz V
T-1179	10	900	24	2	31	Amp Cpx L V
T-1180	10	850	288	2	31	Amp Anr L V
T-1189	5	900	91	2	22	Amp Anr Opx L V
T-1190	5	850	164	2	19	Amp Anr Opx L V
T-1200	10	950	23	2	23	Opx Cpx L V
T-1223	5	950	27	3	21	Opx L V
T-1224	5	800	169	3	22	Amp Anr Qtz V
T-1230	10	950	67	3	19	Opx Cpx L V
T-1350	5	850	73	6	22	Crd Opx L V
T-1371	5	825	119	5	23	Amp Anr L V
T-1374	5	800	139	5	22	Amp(?) Anr Qtz L V
T-1388	5	800	266	6	20	Crd Opx Anr L V
T-1392	10	750	18	Talc oxides	20	Talc
T-1396	17	850	125	3	19	Amp Qtz V
T-1397	10	770	214	5	13	Amp Qtz L V
T-1398	5	850	214	5	20	Amp Anr L V
T-1403	10	975	169	4	2	Opx Cpx L
T-1415	10	925	569	4	2	Opx Cpx L
T-1444	10	900	216	4	2	Amp Anr Qtz
T-1446	5	900	120	4	2	Amp+?
T-1487	5	950	195	4	2	Anr Opx Cpx L
AT-142	0	1215	97	6	0	Anr Opx Crd Qtz
AT-142	0	1215	97	2	0	Anr Opx Qtz L
AT-143	0	1225	358	6	0	Anr Opx Crd Qtz
AT-143	0	1225	358	2	0	Anr Opx Qtz L
AT-143	0	1225	358	5	0	Anr Opx Qtz
AT-151	0	1215	47	7	0	Anr Opx Crd Qtz

Z = Zurich; T = Tasmania; AT = 1 atmosphere.

T-1403 to T-1487 were dehydration experiments with water only present in the amphibole.

T-1446: only amphibole was positively identified, although other phases must also be present because of starting mix composition.

Where feasible, both cores and rims of minerals were analysed in order to check for zoning. In those cases where interference from other phases was encountered during analysis, the more stoichiometric analyses were taken as the equilibrium composition. Where zoning or inhomogeneity existed, compositional ranges are reported in the tables of run product compositions.

Liquids in this system quenched to clear glasses devoid of quench crystals or overgrowths to primary crystals. Run products below the solidus were generally friable and easily ground in an agate mortar. The presence of melt corresponded with a much denser sample and a greater difficulty in grinding fragments for optical examination.

Glasses were easily recognized with the SEM microprobe. Both point analyses and area scans of glasses were made to check for homogeneity. Glass analyses totalled between 80 and 90 wt. per cent oxides. The difference from 100 per cent probably does not correspond to the actual water content. Microprobe analyses of glasses with known water contents result

in probe totals whose difference from 100 wt. per cent is in excess of the actual water content (D. H. Green, pers. comm.). The glass analyses reported in Table 5 have been readjusted to 100 wt. per cent anhydrous and original totals are also shown.

4. THE QUARTZ- AND H_2O-SATURATED SOLIDUS AND RELATED SUBSOLIDUS EQUILIBRIA

Stewart's (1967) study of the anorthite + quartz + H_2O eutectic to 10 kb and Boettcher's (1970) study to higher pressures (involving zoisite and kyanite instead of anorthite) provided important limits to the possible quartz- and H_2O-saturated solidus segments in CMASH. MgO enters the anorthite + quartz liquids at higher pressure as it does at 1 atm (for example see the flow charts by Schairer & Yoder, 1970, p. 212 and Humphries, Biggar & O'Hara, 1972, p. 139) and thus any CMASH reaction involving anorthite + quartz + H_2O would lie at a lower temperature than in CASH. Thus, in CMASH, the model solidus could be defined by one or two families of eutectics; depending upon whether Anr + Opx + Cpx + Qtz + H_2O and Anr + Crd + Opx + Qtz + H_2O are eutectic at higher pressures, continually separating peraluminous from sub-aluminous eutectic melts, even though involving different alternative assemblages at higher pressures (e.g. with talc or with zoisite and kyanite). This would be equivalent to the persistence to higher pressures of the apparent quartz–norite thermal divide (Gribble & O'Hara, 1967) at 1 atm (Fig. 3A, B), where Qtz + Opx + Anr separates Cpx from Crd parageneses that O'Hara (1968, p. 71) suggested may be present to 15 kb under water deficient conditions.

4.1 *Near-solidus phase relations in CMAS at 1 atm*

Several workers (see Chinner & Schairer, 1962; Gribble & O'Hara, 1967; O'Hara, 1968; Schairer & Yoder, 1970 (fig. 11)) have suggested that at 1 atm the assemblages Anr + Opx + Cpx + Trd and Anr + Opx + Crd + Trd melt eutectically to subaluminous and peraluminous melts respectively. These subsystems are separated by the Anr + Opx + Trd thermal divide. Experiments performed by us in this system confirm the eutectic melting behaviour of the assemblage Anr + Opx + Cpx + Trd and also that it melts at a lower temperature than the assemblage Anr + Opx + Crd + Trd (Table 4). At 1215 °C the Anr + Opx + Cpx + Trd composition produced abundant glass free from quench-crystals together with Anr + Opx + Qtz. In contrast the Anr + Opx + Crd + Qtz mix was unchanged, apart from the presence of Al_2O_3 in the orthopyroxene. A similar result was obtained at 1225 °C (Tables 4 & 5; Fig. 3). The possibility that a Crd-bearing mineral mix was not melting because of lack of contact between mineral grains was discounted by repeating the 1215 °C experiment using a fused glass of the same composition as the mineral mix. This glass devitrified to Anr + Opx + Crd + Qtz, suggesting that the Cpx-bearing 1 atm eutectic assemblage melts at a lower temperature than the Crd-bearing assemblage. The present experiments also showed that Anr + Opx + Trd had not melted at 1225 °C (Anderson, 1915, had determined the eutectic temperature as 1222 °C) and thus the exact nature of the melting reactions shown in Fig. 3B remains unknown. Either the thermal divide is stable separating the highest T eutectic among Anr + Opx + Crd + Qtz from Anr + Opx + Cpx + Qtz, or the former is peritectic. In either case fractionation of Cpx cannot produce peraluminous derivative liquids.

4.2 *Near-solidus phase relations below 5 kb* P_{H_2O}

The effects of H_2O on the melting reactions in CMASH are poorly known. Yoder (1965) observed that, at 5 and 10 kb P_{H_2O}, the eutectic in diopside–anorthite shifts considerably towards the anorthite composition. In our runs (Tables 4 & 5) a synthetic mineral mixture of

TABLE 5

Mineral and melt compositions for the CMASH experiments

Phase / *Run*	*Amp* *Z-25*	*Amp* *T-1179*	*Amp* *T-1179*	*Cpx* *T-1179*	*Melt* *T-1179*	*Amp* *T-1180*	*Melt* *T-1180*	*Amp* *T-1189*	*Melt* *T-1189*	*Amp* *T-1190*	*Opx* *T-1190*	*Melt* *T-1190*	*Opx* *T-1230*	*Cpx* *T-1230*	*Melt* *T-1230*
P (kb)/*T* (°C)	10/800	10/900				10/850		5/900		5/850			10/950		
SiO_2 (wt per cent)	56·07	54·03	53·01	54·26	64·31	54·65	66·61	56·65	69 17	55·74	57·01	72 52	56 29	53 43	62·76
Al_2O_3	5·72	9·67	11 80	6·51	23·29	10·10	21 49	4 37	18·55	6 97	2·43	17 10	6·34	4·11	24·58
MgO	22·33	22 18	21·38	17·56	1·84	20·95	2·04	23·50	3 25	20·68	37 13	2·69	36 79	19·12	2 14
CaO	12·84	12 82	13·08	23·31	10·56	12·77	9·86	12 34	9·03	11·03	0·27	7 69	0·57	23 15	10·52
Total	96·96				86 95		86·61		88 26			86 28			84·11
Si (atoms)	7 617	7·227	7·057	1·899	4·197	7 305	4·323	7·697	4·469	7 703	1·966	4·641	1·884	1·912	4 106
Al	0·917	1 525	1·852	0·268	1 792	1 591	1·644	0·700	1·412	1·135	0·099	1·290	0·250	0·173	1 895
Mg	4 521	4·422	4·242	0·916	0·179	4 174	0·198	4 760	0·313	4·259	1 909	0·257	1 836	1·020	0·208
Ca	1·869	1·837	1 886	0·874	0·738	1·829	0·686	1 797	0·625	1 633	0·010	0·527	0·021	0·888	0·736
Cation total	14·924	15·011	15·017	3·964	6·907	14·899	6 851	14·954	6·819	14 73	3·984	6 714	3 991	3 993	6·945
No. of oxygens	23	23	23	6	12	23	12	23	12	23	6	12	6	6	12
A (molar)	6 7	10·86	13 13	6·96	49·43	14·0	48·18	5·06	43 45	8·28	2·5	45·14	6 3	4 34	50·04
C	27 3	26·16	26·74	45 42	40·72	26·2	40·21	26·01	37·69	25·28	0·5	36 93	1·0	44 51	38 95
M	66·0	62·97	60·13	47 6	9·85	59·8	11·60	68·92	18·85	65·93	97·0	17·92	92·6	51 14	11·0

Phase / *Run*	*Opx* *T-1350*	*Crd* *T-1350*	*Melt* *T-1350*	*Amp* *T-1371*	*Melt* *T-1371*	*Melt* *T-1374*	*Opx* *T-1388*	*Melt* *T-1388*	*Amp* *T-1396*	*Amp* *T-1397*	*Melt* *T-1397*	*Melt* *T-1398*
P (kb)/*T* (°C)	5/850			5/825		5/800	5/800		17/850	10/770		5/850
SiO_2 (wt per cent)	58·55	51 49	76·52	58·28	75 31	75·62	58·83	75·31	54·95	56·81	74·49	73·77
Al_2O_3	3·47	34·86	14·84	3 76	15 73	15·58	2·02	15 79	9·45	6·44	15·98	15 81
MgO	37·98	13·47	2 91	24·58	2·18	2·28	38·2	2 22	22·31	23·37	1 33	2·01
CaO	0·0	0·17	5·73	12·81	6·78	6·21	0·45	6 54	13·29	13 38	8·19	8·41
Total			87 38		85·58	84·35		86·05			82·06	86·72
Si (atoms)	1 953	5·013	4 839	7·723	4 783	4·800	1·968	4·783	7·259	7·502	4 755	4·722
Al	0·136	4·000	1·106	0·587	1 178	1·166	0·080	1·182	1·472	1·002	1·202	1 192
Mg	1·889	1 955	0·274	4·854	0·206	0·216	1·905	0·210	4 392	4 600	0·127	0·192
Ca	0·000	0·018	0·388	1·819	0·461	0·422	0·016	0·445	1 881	1 894	0·560	0·577
Cation total	3·978	10·986	6·607	14 983	6·628	6·604	3·969	6 620	15·004	14·998	6·444	6·683
No of oxygens	6	18	12	23	12	12	6	12	23	23	12	12
A (molar)	3·47	50·34	45·51	4·21	46·84	47 7	2·04	47·4	10·5	7·16	46·7	43·66
C	0·00	0·45	31 93	26·11	36 73	34·6	0·82	35·7	26·84	27·08	43·5	42·27
M	96·53	49 21	22 55	69·68	16·43	17·7	97 14	16·85	62 66	65 76	9 9	14·07

Phase / *Run*	*Opx* *T-1403*	*Cpx* *T-1403*	*Melt* *T-1403*	*Opx* *T-1415*	*Cpx* *T-1415*	*Melt* *T-1415*	*Amp* *T-1444*	*Opx* *T-1487*	*Melt* *T-1487*	*Opx* *AT-142/2*	*Melt* *AT-142/2*	*Opx* *AT-142/6*	*Opx* *AT-143/2*	*Melt* *AT-143/2*
P (kb)/*T* (°C)	10/975			10/925			10/900	5/950		0/1215		0/1215	0/1225	
SiO_2 (wt per cent)	58 28	55·31	67·72	58·09	54·30	67·82	54·62	59·08	66·38	60·22	62 81	61·29	58 78	62 73
Al_2O_3	2·98	2·26	18 34	3 52	2·64	18·54	9·75	1·43	19 28	0·54	15·30	2 18	2 54	15 90
MgO	37·80	20·23	3 75	31·68	19·05	3 76	22 10	38·68	3·61	38·59	8·30	36·32	37·35	8·74
CaO	0·94	22·19	10·19	0·71	24·01	9·88	13 54	0·81	10·73	0·65	13 59	0·21	1 32	12 63
Total			93·74			84·27			87·69		99·95			100·0
Si (atoms)	1·952	1·969	4·408	1·944	1 947	4·409	7 223	1 978	4·336	2·012	4·196	2·031	1·969	4 179
Al	0·118	0·095	1·407	0·139	0·112	1·420	1 519	0·056	1·484	0·021	1·205	0·085	0·100	1 248
Mg	1·886	1·074	0·364	1·879	1·018	0·364	4·356	1 930	0·351	1·921	0·826	1·797	1·865	0·868
Ca	0·034	0·846	0·710	0·026	0·922	0·688	1·919	0·029	0·751	0·023	0·973	0·007	0·047	0·901
Cation total	3·990	3 984	6 889	3·988	3 999	6·881	15·017	3·993	6·922	3·977	7 201	3·923	3·981	7·196
No. of oxygens	6	6	12	6	6	12	23	6	12	6	12	6	6	12
A (molar)	2 98	2·41	39 6	3·52	2·81	40·3	10·80	1 4	40·2	0·54	22 5	2·30	2·55	26·07
C	1·72	43·00	39·9	1·32	46·19	39 1	27 28	1·4	40·7	1·18	41 87	0·38	2·40	37·65
M	95·30	54 59	20·5	95·16	51·00	20·7	61 92	97 1	19·1	98 29	35·59	97·32	95·06	36·27

Melt compositions have been readjusted to 100 per cent with original probe totals also shown (see text).

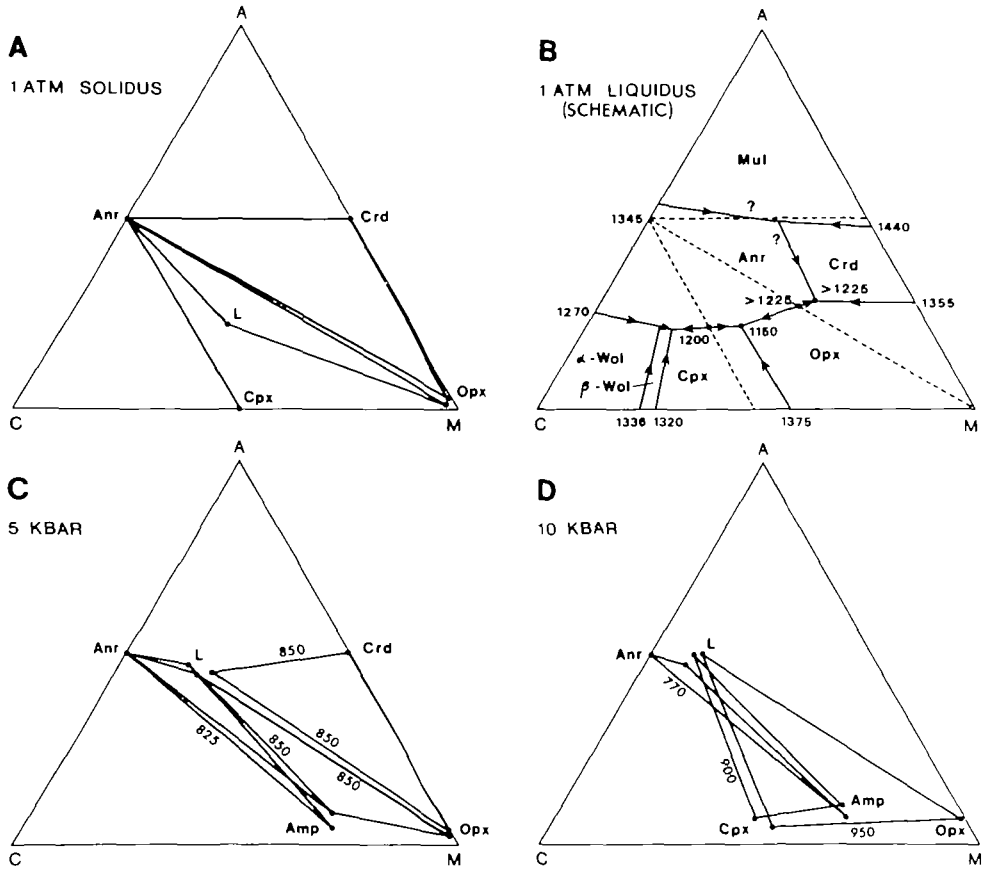

FIG. 3. Isobaric polythermal sections showing the coexisting phases synthesized from the various starting compositions on ACM projections from Qtz+H_2O at 1 atm (A), 5 kb P_{H_2O} (C) and 10 kb P_{H_2O} (D). A schematic diagram for the tridymite saturated liquidus for 1 atm is also shown in B constructed from data on the boundary systems presented by Osborn & Muan (1960), Anderson (1915), Chinner & Schairer (1962), and from the present study. Temperatures are shown on tie-lines (and it should be noted that quartz is exhausted by melting from some of these compositions).

Anr + Ens + Qtz produced a peraluminous liquid at 5 kb P_{H_2O} from 800 to 850 °C (Fig. 3). This peraluminous liquid coexists with diopsidic-Cpx at high temperature, and amphibole plus anorthite at lower temperature. Thus it appears that at water saturation in CMASH, the apparent quartz-norite thermal divide has disappeared by 5 kb and permits diopside-normative rocks to produce an initial peraluminous melt.

Two possible sets of phase relations pertaining to the behaviour of the quartz-norite divide under water-saturated conditions are shown in Fig. 4. The topologies of the reactions depend upon whether the singular point, S, occurring when the eutectic reaction

$$\text{Anr} + \text{Opx} + \text{Qtz} + \text{V} = \text{L} \tag{10}$$

intersects the appropriate solidus above or below the invariant point I. For case (A) where the singular point occurs below the invariant point, the reaction among Anr + Cpx + Opx + Qtz + V + L changes from eutectic:

$$\text{Anr} + \text{Opx} + \text{Cpx} + \text{Qtz} + \text{V} = \text{L} \tag{11}$$

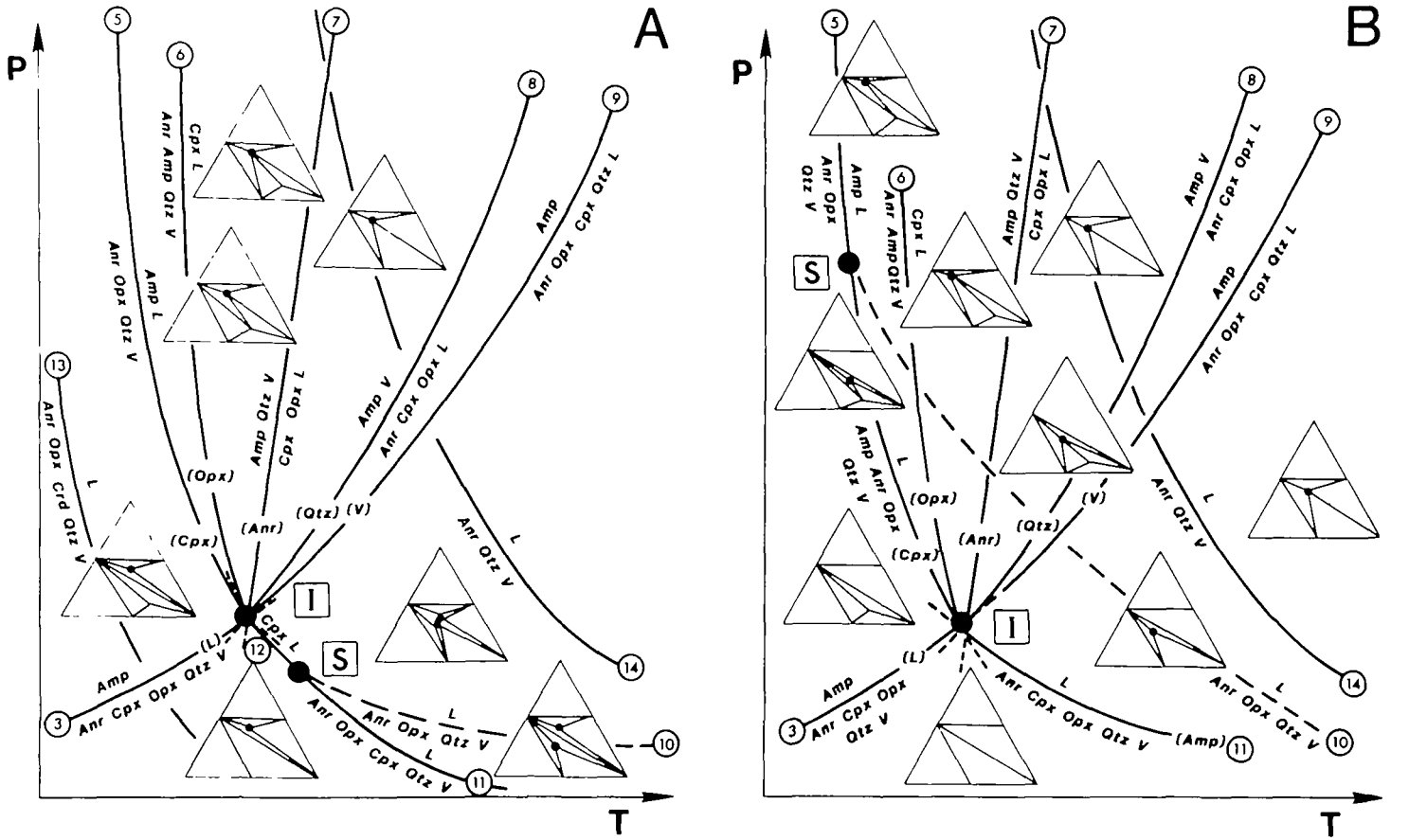

FIG. 4. Schematic P–T diagrams showing alternatives for the generation of peraluminous melts below 5 kb P_{H_2O}, depending upon whether the singular point [S], which is generated by the intersection of the eutectic reaction (10) Anr + Opx + Qtz + V = L with other quartz- and water-saturated solidi, occurs at lower (Fig. 4A) or at higher (Fig. 4B) pressures than the invariant point [I]. Case (A) represents the generation of peraluminous melts in model mafic compositions at low pressures through the change of Cpx from congruent (Anr + Opx + Cpx + Qtz + V = L (11)) to incongruent (Anr + Opx + Qtz + V = Cpx + L (12)) melting. Case (B) represents a change at higher pressures of amphibole from congruent (Anr + Opx + Amp + Qtz + V = L (15)) to incongruent (Anr + Opx + Qtz + V = Amp + L (5)) melting. Triangles depict stable assemblages (liquid as a heavy dot) on an ACM projection from Qtz and H_2O (see Figs. 2A and 3). Although we cannot distinguish between (A) and (B) on available evidence Figs. 5 and 6 are drawn only for case (A) topology.

to peritectic below about 2 kb P_{H_2O} (Fig. 5), that is:

$$\text{Anr} + \text{Opx} + \text{Qtz} + \text{V} = \text{Cpx} + \text{L}. \quad (12)$$

Under these circumstances (Fig. 4A) the lowest temperature melting reactions in CMASH at quartz- and H_2O-saturation will be an eutectic among Anr + Opx (or talc) + Qtz + H_2O and an aluminous phase (cordierite or kyanite) in a pseudo-pelitic system. The first liquids produced in pseudo-basaltic compositions will be peritectic through Anr + Opx (or talc) + Qtz + H_2O melting to Cpx or Amp with a peraluminous liquid (Fig. 4A).

For the case in Fig. 4B where the singular point, S, occurs at pressures above the invariant point, the eutectic reaction at low pressures:

$$\text{Amp} + \text{Anr} + \text{Opx} + \text{Qtz} + \text{V} = \text{L} \quad (15)$$

becomes peritectic at higher pressures:

$$\text{Anr} + \text{Opx} + \text{Qtz} + \text{V} = \text{Amp} + \text{L}. \quad (5)$$

Under these circumstances (Fig. 4B) the apparent quartz–norite divide persists to some pressure between 2 and 5 kb P_{H_2O}. However, in either case, the peritectic reactions above the solidus have the same topology, differing only in the peraluminous (corundum-normative) or subaluminous (diopside-normative) nature of the early liquids. It will be noted that in case (A) two eutectic liquid fields coalesce at a saddle point on the Anr + Opx + Qtz + H_2O join, whereas in case (B) the eutectic liquid produced from Anr + Opx + Cpx + H_2O melting simply enlarges to more aluminous compositions as Anr + Opx + Qtz + H_2O melts.

Microprobe analyses (Table 5) of the melts produced at 5 kb P_{H_2O} from amphibolite are clearly peraluminous (Figs. 2A, 3C). However, since the three reactions involving respectively Crd, Amp and Cpx with Anr + Opx (or Tal) + Qtz + H_2O occur within a temperature interval of less than 25 °C, available data are not adequate to constrain the extremely complex phase relations postulated here (Figs. 5 & 6). These consistent topologies should help direct any future experiments on these reactions. The data are adequate, however, to demonstrate that the quartz-norite thermal divide possibly occurring at 1 atm, has certainly disappeared by 5 kb P_{H_2O}. Note the similarity in compositions of melts formed at 5 kb P_{H_2O} from aluminous (Anr + Opx + Crd + Qtz + H_2O) and mafic (Anr + Opx + Cpx + Qtz + H_2O) starting compositions in which Crd and amphibole respectively occur with liquid (Table 5, Fig. 3C).

4.3 *Near-solidus phase relations from 5 to 10 kb* P_{H_2O}

The present results at P_{H_2O} = 5 kb correlate with other runs at 10 kb (Fig. 5 and Tables 4 & 5) in that the CMASH reactions relevant to model amphibolite melting:

$$\text{Anr} + \text{Opx} + \text{Qtz} + \text{V} = \text{Amp} + \text{L} \quad (5)$$

and

$$\text{Anr} + \text{Amp} + \text{Qtz} + \text{V} = \text{Cpx} + \text{L} \quad (6)$$

occur between 800 °C and 825 °C at 5 kb and both below 800 °C at 10 kb P_{H_2O}, although Zoi enters into the melting reactions. The disappearance of an aluminous amphibole in CMASH with excess quartz and H_2O according to the reaction:

$$\text{Amp} + \text{Qtz} + \text{V} = \text{Cpx} + \text{Opx} + \text{L} \quad (7)$$

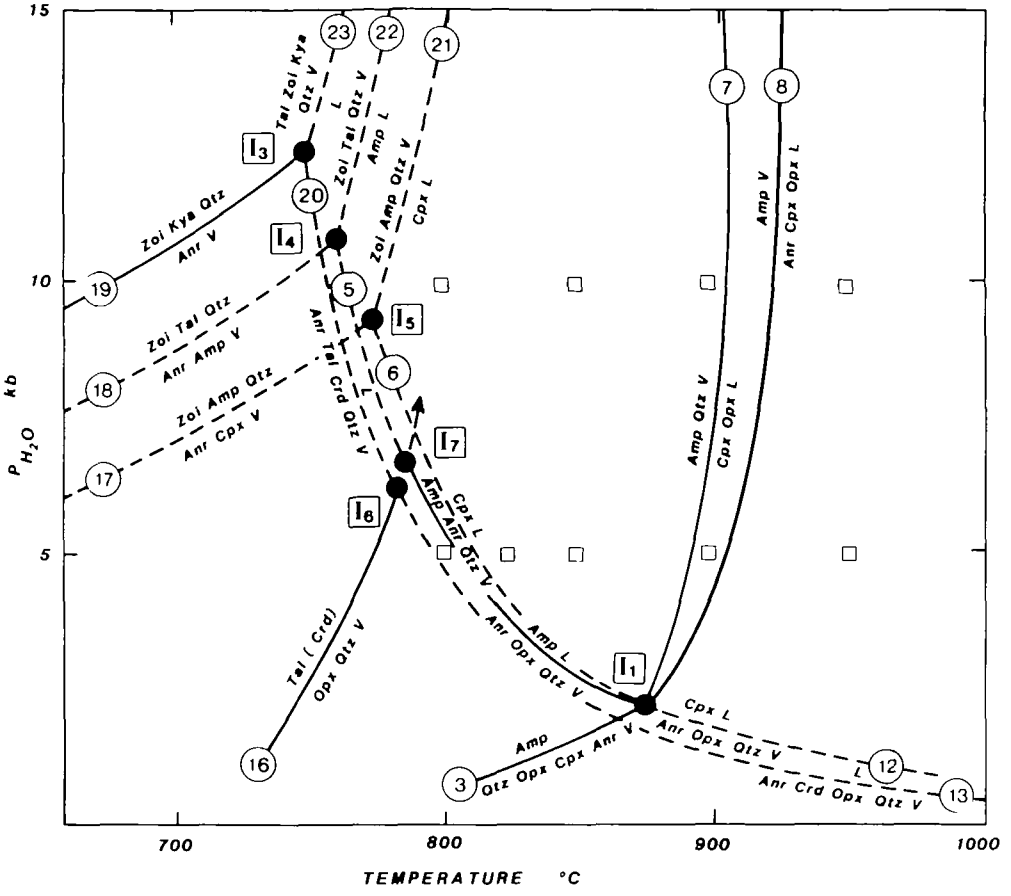

FIG. 5. H_2O-excess phase relations deduced from the present experiments and those of other workers, plus those inferred from topological arguments. The open squares show the P–T conditions of experiments and the labelling of curves corresponds to Fig. 4A (invariant point I_1 = I) and Table 2.

occurs between 850 and 900 °C at 5 kb and 900 and 950 °C at 10 kb P_{H_2O} (Fig. 5) and 15 kb P_{H_2O} (Ellis & Thompson, in prep.). Runs from which quartz had disappeared permitted location of the reaction:

$$\text{Amp} + \text{V} = \text{Anr} + \text{Cpx} + \text{Opx} + \text{L} \quad (8)$$

between 900 and 950 °C at 5, 10 and 15 kb P_{H_2O}.

4.4 *Subsolidus phase relations between 5 and 15 kb*

The addition of MgO to the solidus phase relations presented for CASH by Boettcher (1970, fig. 4) means that the near-solidus phase relations are much influenced by the planes Anr-Opx, Anr-Tal and Zoi-Tal (each with Qtz and H_2O) with increasing pressure in the subsolidus region. The above interpretations (Fig. 4A or B) of the low pressure disappearance of the quartz-norite divide at quartz- and H_2O-saturation means that the lowest temperature melting will be eutectic, as shown schematically in Fig. 6.

In the subsolidus region, zoisite will first appear in percalcic compositions (through

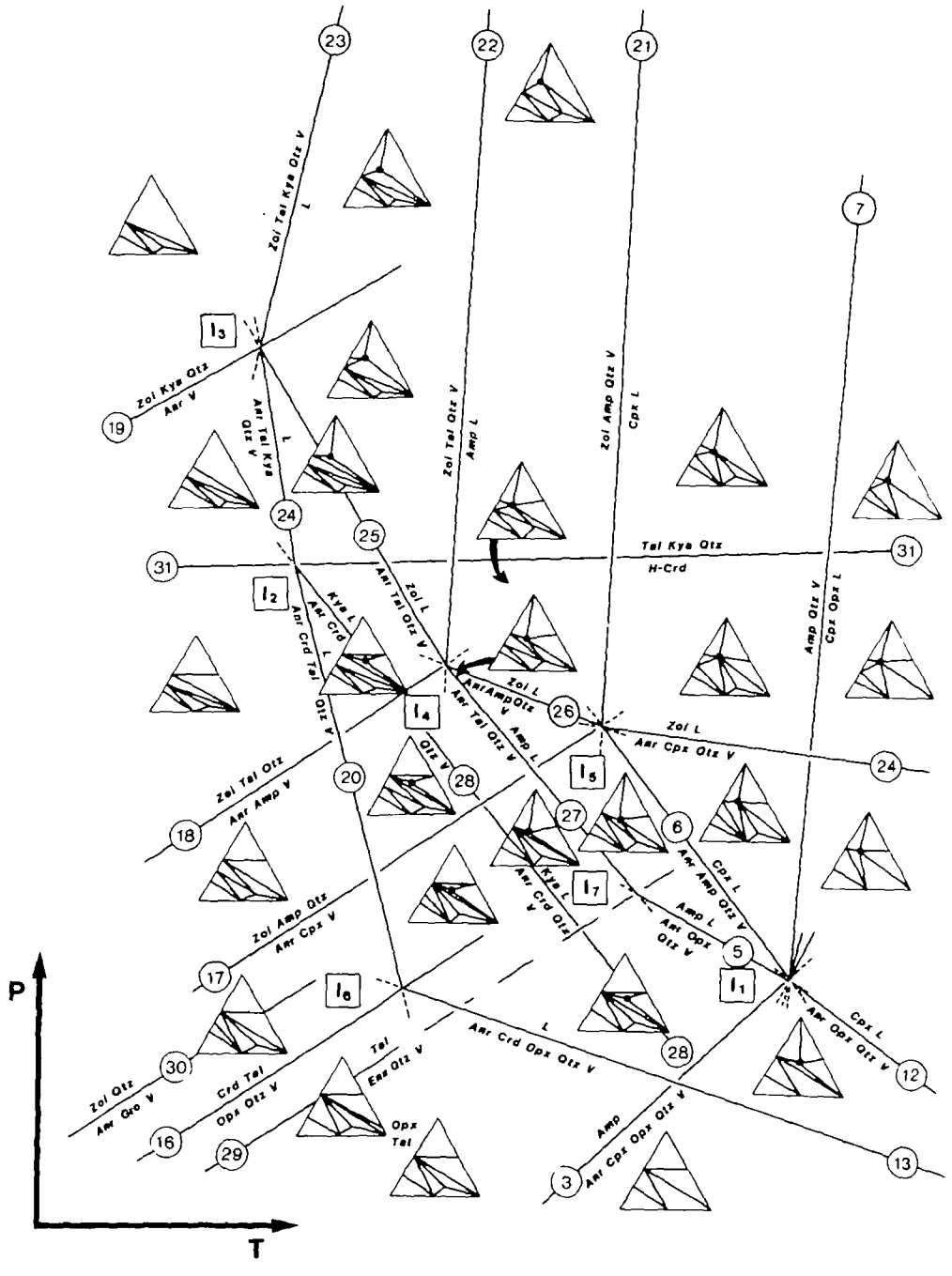

FIG. 6. A schematic P-T diagram showing the evolution of peraluminous melts in CMASH assuming case (A) of Fig. 4 where the lowest temperature eutectic melting involves Anr + Crd + Opx, Anr + Crd + Tal and Anr + Kya + Tal (each with Qtz and H_2O) with increasing pressure. Triangles represent an ACM projection from Qtz + H_2O depicting stable assemblages in which melts are shown by dots (see Figs. 3 & 4). The diagram is easily calibrated in P-T space by reference to Fig. 5.

Anr + Gro + V = Zoi + Qtz (3)) and will occur in model basaltic compositions through the reactions similar to:

$$\text{Anr} + \text{Cpx} + \text{V} = \text{Zoi} + \text{Amp} + \text{Qtz} \tag{17}$$

and

$$\text{Anr} + \text{Amp} + \text{V} = \text{Zoi} + \text{Tal} + \text{Qtz}. \tag{18}$$

Neither of these subsolidus reactions (17) and (18) have been located exactly from the present experiments. The subsolidus reaction in CASH

$$\text{Anr} + \text{V} = \text{Zoi} + \text{Kya} + \text{Qtz} \tag{19}$$

stabilizes the join Zoi + Tal (+ Qtz + H_2O). The computed curve (Essene *et al.*, 1973, in Vernon, 1976, fig. 4.12; and Delaney & Helgeson, 1978, fig. 7) for:

$$\text{Tal} = \text{Ens} + \text{Qtz} + \text{V} \tag{29}$$

cuts the solidus at about 780 °C–800 °C at 5–6 kb, although the actual reactions will also include aluminous enstatite in MASH, e.g.

$$\text{Tal} + \text{Crd} = \text{Opx} + \text{Qtz} + \text{V} \tag{16}$$

(Newton, 1972, fig. 8). The MSH breakdown reaction has been used here (Figs. 5 & 6) to minimize further complications. The postulated solidus is further affected by the breakdown of hydrous cordierite (H-Crd) to Ens + Al_2SiO_5 + Qtz + H_2O (Newton, 1972, fig. 9) which is shown here with talc instead of enstatite near 11 kb, invariant point I_2 (Fig. 6). Newton (1972, p. 403) remarked that even in the MASH system, the reaction of Tal + Sil + Qtz = Crd + V is interrupted near 800 °C at about 11 kb P_{H_2O} by the onset of melting and the development of Opx + Sil + Liquid.

4.5 *Near-solidus phase relations above 10 kb* P_{H_2O}

At pressures above about 12 kb the assemblage Zoi + Kya + Qtz replaces Anr + V in CASH along the solidus (Figs. 1 & 5); the appropriate solidus reaction in CMASH is deduced here to be:

$$\text{Zoi} + \text{Tal} + \text{Kya} + \text{Qtz} + \text{V} = \text{L}. \tag{23}$$

The other reactions above the solidus in the quartz- and H_2O-saturated portion of CMASH in the region of 10 to 15 kb are also complicated by the replacement of Anr by Zoi + Kya. Two additional invariant points (I_4 among Zoi + Tal + Anr + Amp + Qtz + L + V; and I_5 among Zoi + Cpx + Anr + Amp + Qtz + L + V) have been deduced from available data (Figs. 5 & 6). These invariant points limit the coexistence of Anr + Amp + Qtz + H_2O in CMASH to a region bounded by the invariant points I_1, I_5, and I_4 and the two appropriate subsolidus reactions (3) and (18). At pressures above the univariant dehydration reaction (19) and invariant points I_3, I_4, and I_5, the breakdown reactions

$$\text{Zoi} + \text{Tal} + \text{Qtz} + \text{V} = \text{Amp} + \text{L} \tag{22}$$

$$\text{Zoi} + \text{Amp} + \text{Qtz} + \text{V} = \text{Cpx} + \text{L} \tag{21}$$

replace (27) and (6), involving Anr.

5. THE DISAPPEARANCE OF QUARTZ AND THE COMPOSITION OF THE WATER-SATURATED MELTS

Many of the experiments, even though starting with quartz in greater amount than normally found in amphibolites, lost quartz at or just beyond water-saturated melting. This occurs because the melts are all very siliceous; compare the Anr + Qtz + H_2O eutectic compositions (from Stewart, 1967, fig. 8) with the present melt compositions projected from $CaMgSi_2O_6$ and H_2O in Figs. 2B and 7. All H_2O-excess melts up to 950 °C at all pressures are peraluminous and plot below the $CaAl_2SO_6 + Mg_2SiO_4 + SiO_2$ plane in Fig. 2B. Although some of the melts shown in the ACM diagram in Fig. 2A are projected from SiO_2, the absence of quartz in these run products does not change their peraluminous nature, as mass balance calculations show them to have Al in excess of Anr + aluminous Opx.

The apparent movement of the liquid compositions with pressure towards Anr and away from Opx in the ACM projection from SiO_2 and H_2O (Fig. 2A) and towards Anr and away from Qtz in the Cats + For + Qtz projection from Dio and H_2O (Fig. 7) can be related to the buffering reaction discussed above:

$$CaAl_2Si_2O_8\ [Anr] = CaMgSi_2O_6\ [Cpx\ or\ Opx] + Al_2Mg_{-1}Si_{-1}\ [Cpx, Opx, Amp\ or\ L] + SiO_2\ [Qtz]$$

Unfortunately, the data are not complete enough to warrant a meaningful calibration of the buffer.

Compared to the Anr + Qtz + H_2O eutectics of Stewart (1967), which are 'illegally' plotted in Figs. 2B & 7 because they do not represent the eutectic with Dio, the CMASH melts are all offset towards Ens on a Dio + H_2O projection (Fig. 7). At both 5 and 10 kb P_{H_2O} there is an increase in Anr relative to Qtz in the liquids with increasing temperature. The 5 kb liquids are more Qtz-rich than the 10 kb liquids at any given temperature.

5.1 *The transition from corundum-normative to diopside-normative liquids*

In the lower pressure region (below 10 kb) where Anr + Opx (or Talc) are involved in melting reactions, the liquids are clearly peraluminous in the conventional sense, up to at least 950 °C. As illustrated by the ACM projected compositional triangles in Figs. 2B, 4 & 6, the melts from model basaltic compositions remain peraluminous at least until they coexist with Cpx + Amp (in this projection from SiO_2 and H_2O). Presumably with further increase in temperature the melts may extend to metaluminous or subaluminous (diopside-normative) compositions. The change from corundum- to diopside-normative may happen with Cpx + Amp + L or with Cpx + Opx + L. Certainly at 1 atm the melts are eutectic to Anr + Opx + Cpx + Trd (Fig. 3A) and therefore diopside-normative. Helz (1976), in her study of basalt (amphibolite) melting at 5 kb P_{H_2O}, also produced peraluminous melts for the first 300 degrees of melting. At about 1025 °C the melts changed from corundum- to diopside-normative (Fig. 10). Conversely, Cawthorn & Brown (1976) and Cawthorn & O'Hara (1976) showed that amphibole fractionation from calc-alkaline/basaltic compositions may lead to peraluminous later derivatives. However, this in itself cannot produce peraluminous liquids as it also requires the breaking of the quartz–norite thermal divide as shown here experimentally.

Progressive melting of model amphibolite in CMASH leads to lower H_2O, Al_2O_3, and SiO_2 in the liquids at successively higher temperatures at constant pressure. To permit forsterite to coexist with these hydrous melts in CMASH, Anr + Cpx + Opx must become unstable (as in the anhydrous system) and amphiboles must be absent or very tschermakitic (Fig. 2B). This situation is favoured at very low pressures where amphibole is no longer stable, or at higher pressures where garnet is stable.

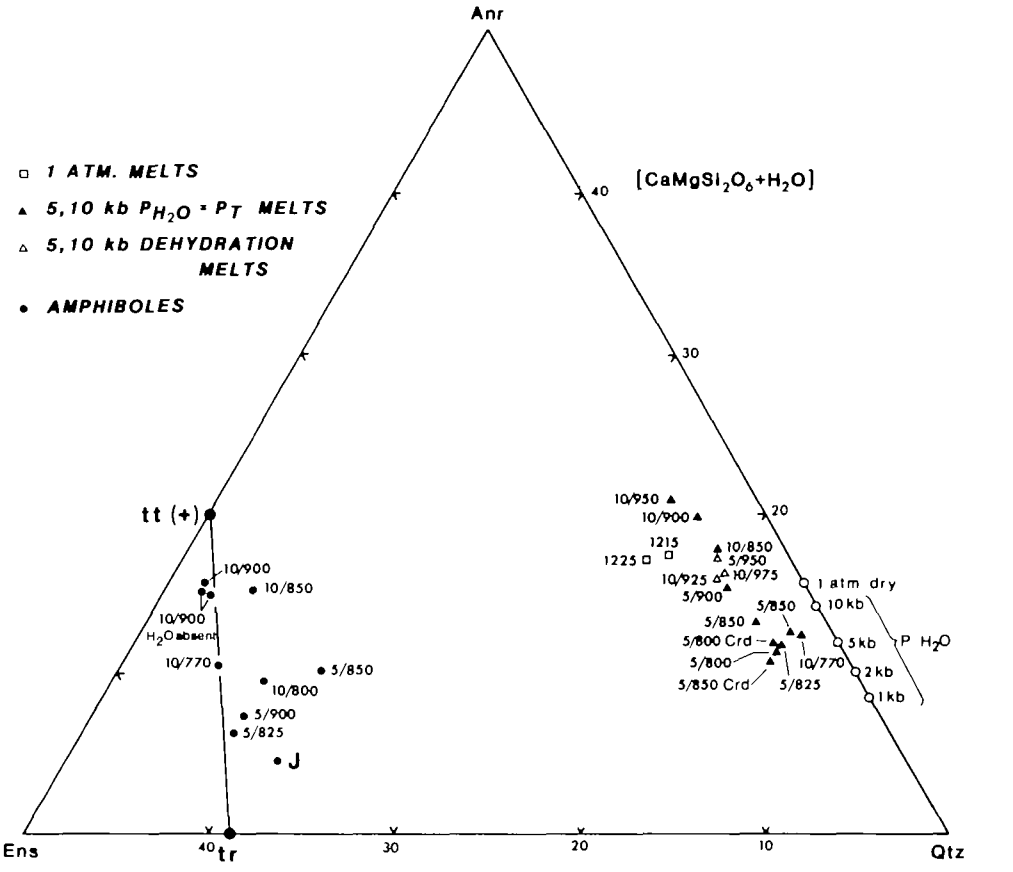

FIG. 7. An expanded portion of Fig. 2B. The water-excess melt compositions lie below the plane (negative diopside) and their evolution may be compared with the results on the Anr-Qtz-H_2O eutectic (open circles) from Stewart (1967, fig. 8). Melts formed by V-absent dehydration melting of Amp+Qtz assemblages and 1 atm melts lie above the plane (positive diopside). Experimentally-produced amphiboles are also shown together with aluminous tremolite (J) from the For-bearing CMASH experimental study by Jenkins (1981). In the Qtz-excess experiments there is a clear increase in $Al_2Mg_{-1}Si_{-1}$ in the amphiboles with increase in both pressure and temperature, though none are more aluminous than Tt. Pressure and temperature (kb/°C) for each melt is also shown. Melts formed from peraluminous starting composition are additionally labelled with Crd.

6. AMPHIBOLE IN SILICA-UNDERSATURATED COMPOSITIONS IN CMASH

As shown in Fig. 2B, tschermakitic amphiboles are more likely to coexist with For than Qtz in CMASH (see also Obata & Thompson, 1981; Jenkins, 1981, 1983). In the presence of For, Amp does not coexist with melt in the CMASH system. In his experimental study of Anr + For + Opx + V in the proportions of tschermakite (Ts) = (2 Anr + For + Ens + H_2O), Oba (1978, p. 343) did not observe Amp coexisting with melt. Ford *et al.* (1977) did not observe Amp on the solidus in their study of the H_2O-saturated model peridotite solidus in CMASH. Jenkins (1981, 1983) has shown that, in the For-excess CMASH system, Amp dehydrates at least 150 °C below the H_2O-excess peridotite solidus.

In contrast to the results of Oba (1978) who considered that pure Ts ($Ca_2Mg_3Al_4Si_6O_{20}(OH)_2$) is stable with respect to the assemblage Anr + Opx + For + V at around 850 °C, the experiments and probe data of Jenkins (1981, 1983) show that the synthesized amphiboles only contain about 20-30 mol per cent Ts (i.e. Tr-Tt rather than Tt-Ts solid solution)

in For-bearing assemblages (point J in Fig. 7). It therefore appears that, up to 15 kb, Amp in the CMASH system is less aluminous than Tt for both Qtz-excess and For-excess assemblages.

This limited $Al_2Mg_{-1}Si_{-1}$ exchange in amphiboles provides an explanation of why amphibole intersects the H_2O-saturated solidus in Qtz-excess but not in For-excess CMASH systems. Thus, for amphiboles less aluminous than Tt the dehydration reactions are written as:

$$\text{Amp} = \text{Anr} + \text{Cpx} + \text{Opx} + \text{Qtz} + \text{V} \tag{3}$$

and

$$\text{Amp} + \text{For} = \text{Anr} + \text{Cpx} + \text{Opx} + \text{V}. \tag{4}$$

The terminal reaction (3) defines the maximum stability of Amp as being with excess Qtz (above the CMASH H_2O-saturated solidus) whereas the presence of For reduces the stability field of Amp so that it dehydrates below the For-excess CMASH solidus.

In his study of Anr + For + H_2O, Yoder (1966) indicated a melting reaction (For-absent) involving Amp + Anr + Cpx + Opx + Spn + H_2O between 900 and 920 °C at 10 kb P_{H_2O} (see Fig. 8). This means that, in silica-undersaturated but For-absent assemblages in CMASH, Amp intersects the H_2O-saturated solidus near 10 kb. Ford (1976, p. 271), in his

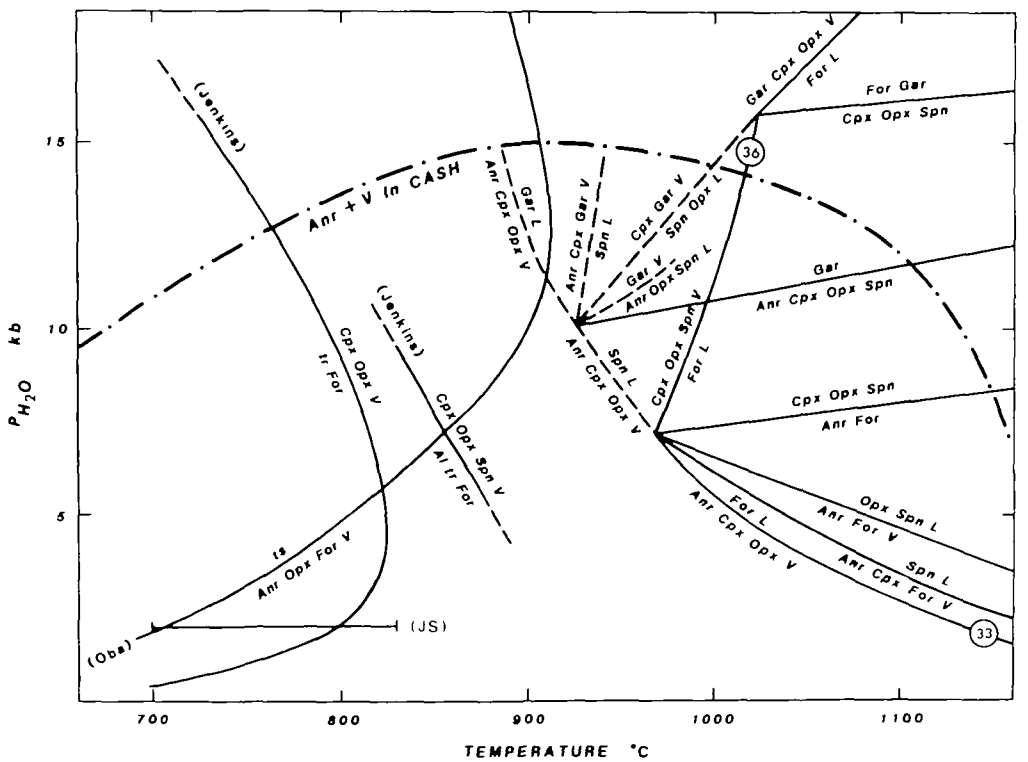

FIG. 8. A *P–T* diagram showing a proposal for the silica-undersaturated (with For and Spn) but water-saturated phase relations in CMASH, deduced from the data of Yoder (1966) and Ford (1976). The stability of tschermakite (Ts) relative to Anr + For + H_2O from Oba (1978) does not appear to intersect the For-bearing solidus, nor does the stability of tremolite (Tr–Tt) relative to Opx + Cpx + Spn + V of Jenkins (1983). In contrast, the data of Yoder (1966) and Ford (1976) indicate a melting reaction near 900–920 °C at 10 kb P_{H_2O} in the absence of For. The bar at 2 kb labelled JS represents the temperature range over which Jasmund & Schäfer (1972) obtained Amp + For + Anr + Opx + H_2O from a tschermakite composition. The upper stability of Anr + V in CASH is from Boettcher (1970).

re-examination of Yoder's (1966) results, concluded that the melting reaction involved Amp + Anr + Cpx + Sap (sapphirine) + H_2O. These results are shown in Fig. 8 (ignoring for simplicity the field of Sap) together with the anhydrous peridotite transitions (from Wood & Holloway, 1984), the stability limit of Anr + H_2O (V) in CASH from Boettcher (1970, Fig. 4), the results of Oba (1978), Jenkins (1981, 1983) and the results at 2 kb P_{H_2O} from Jasmund & Schäfer (1972, fig. 1), who observed Amp + For + Anr + Opx + H_2O obtained from tschermakite composition from about 700 °C to 820 °C.

The compositions of melts produced from water-saturated silica-undersaturated assemblages in CMASH are not easy to predict from available data. The phase diagram presented by Ford *et al.* (1977, fig. 1) implies that not only are the liquids siliceous (from incongruent melting of Opx with Cpx + H_2O and Anr *or* Spn (spinel)) but that from about 6 to 11 kb P_{H_2O}, they are peraluminous as well. Yoder's (1970) study of the join diopside–pyrope–H_2O at 10 kb P_{H_2O} has shown that the beginning of melting of the assemblage For + Opx + Cpx + Spn occurs at about 1000 °C, a temperature similar to that obtained by Jenkins (1983). Kushiro & Yoder (1972) analysed the glasses from three of Yoder's (1970) 10 kb P_{H_2O} run products that coexist with For + Cpx. The glass formed at 1025 °C from two different compositions ($Dio_{45}Pyr_{55}$ and $Dio_{40}Pyr_{60}$) is corundum-normative. The generation of liquids with excess aluminium which coexist with Cpx + For indicates that the join Anr + For + Opx is penetrated by the tie-line Cpx–Melt below 10 kb P_{H_2O} (Kushiro & Yoder, 1972).

The fact that the join Anr + For + Opx + H_2O is crossed at pressures below the invariant point (Fig. 8) with Spn and Cpx at 975 °C and 7·5 kb (Ford *et al.*, 1977, fig. 1), indicates that Cpx enters into a reaction relationship with the liquid through a singular point intersection before the appearance of Spn. Thus, the water-saturated CMASH peridotite solidus must change from

$$\text{Anr} + \text{Cpx} + \text{Opx} + \text{H}_2\text{O} = \text{For} + \text{L} \tag{33}$$

to

$$\text{Anr} + \text{Opx} + \text{H}_2\text{O} = \text{Cpx} + \text{For} + \text{L} \tag{34}$$

in the vicinity of 6 kb and 990 °C.

The model water-saturated peridotite solidus passes from corundum- to diopside-normative near about 11 kb, according to the diagram of Ford *et al.* (1977, fig. 1). This indicates a singular point intersection where the reaction among Spn + For + Opx + V + L induces Cpx out of reaction relationship near this pressure. This means the reaction changes from:

$$\text{Opx} + \text{Spn} + \text{V} = \text{Cpx} + \text{For} + \text{L} \tag{35}$$

at a pressure between 7 and 11 kb (Fig. 8) to:

$$\text{Opx} + \text{Spn} + \text{Cpx} + \text{V} = \text{For} + \text{L} \tag{36}$$

at higher pressures. According to the experimental data of Kushiro (1972), the hydrous liquids coexisting with For, Cpx, and Opx in the CMASH system at 20 kb do not contain excess alumina.

Clearly the phase relations at For and H_2O saturation shown in Fig. 8 are incomplete. However, they emphasize that, in CMASH at least, the attainment of peraluminous composition is caused by reaction relationships with Cpx and not Amp when at For and H_2O saturation. This may be viewed otherwise by remembering that Cpx reaction relationships drive the melts from diopside- to corundum-normative compositions before saturation with spinel is achieved.

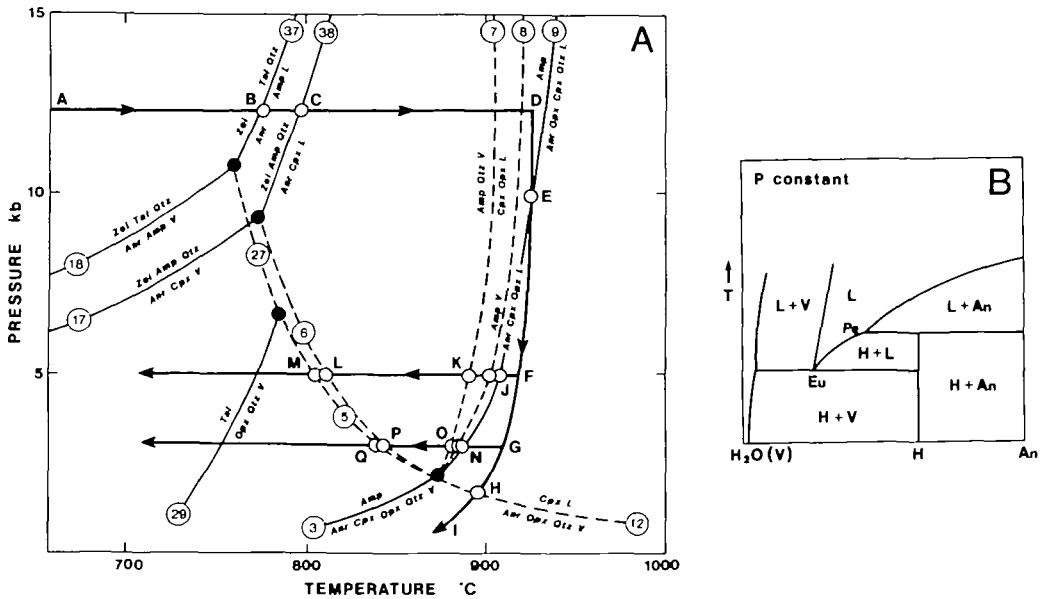

FIG. 9. Dehydration and dehydration-melting reactions in CMASH used to model amphibolite melting. In (A) an arbitrary isobaric heating path beginning at A could undergo dehydration melting at B or C if Zoi + Tal + Qtz or Zoi + Amp + Qtz respectively were present. Dehydration melting of amphibolite would begin at E for the chosen path and the cooling paths illustrate how the final assemblage depends upon the depth of crystallization and ability of water to escape In (B) simplified melting reactions in a binary system are illustrated. This differs from Eggler (1978, p. 332) where a hydrate was also considered to melt congruently, or through the eutectic An + H → L where the melt would be required to contain less H_2O than the hydrate.

7. DEHYDRATION-MELTING REACTIONS IN CMASH AND THE GENERATION OF MELTS IN THE H_2O-UNDERSATURATED REGION

The melting relations discussed so far apply to the water excess region and it is necessary to consider where in P–T space melting will occur if water is not present in excess. With regard to the schematic isobaric T–X section between anhydrous phases (An), an hydrous mineral (H) and H_2O (V), shown in Fig. 9B, the lowest temperature melts would be produced at water saturation through the simplified eutectic reaction H + V = L at point Eu. Any proportions of H and V would yield eutectic melts at water saturation, but for initial proportions of V less than Eu, the melt would become water-undersaturated with further increase in temperature. Most experimental studies of the water-undersaturated region (e.g. Sekine *et al.*, 1981, fig. 2) deal with compositions of H + V approaching H, but do not consider the water-deficient region An + H (exceptions are Brown & Fyfe, 1970; Green, 1973), although such experiments are not made without difficulty (see Helz, 1982, p. 306). We will attempt to consider theoretically the water-deficient region in CMASH and peritectic reactions of the type H = An + L at Pe (Fig. 9B) in the model system. Zoisite, talc, and amphibole are all capable of undergoing dehydration melting to yield water-undersaturated liquidus (Fig. 9). The positions of reactions:

$$\text{Zoi} + \text{Tal} + \text{Qtz} = \text{Anr} + \text{Amp} + \text{L} \tag{37}$$

and

$$\text{Zoi} + \text{Amp} + \text{Qtz} = \text{Anr} + \text{Cpx} + \text{L} \tag{38}$$

are somewhat constrained by the present experimental results with excess water, and the

probable dehydration of talc (see Fig. 1). The curve denoting the dehydration melting of Amp in CMASH at these pressures, i.e.

$$\text{Amp} = \text{Anr} + \text{Opx} + \text{Cpx} + \text{Qtz} + \text{L} \quad (9)$$

must lie at higher temperatures than the quartz-absent but water-excess reaction

$$\text{Amp} + \text{V} = \text{Anr} + \text{Cpx} + \text{Opx} + \text{L} \quad (8)$$

if the subsolidus reaction (3) has Qtz as a product and not as a reactant.

Dehydration melting experiments were undertaken on an aluminous tremolite ($Ca_2Mg_4Al_2Si_7O_{22}(OH)_2$) plus quartz mix (Tables 3 & 4) which was run subsolidus with excess water at 17 kb, 850 °C (Table 3, run T-1396). The aluminous tremolite + Qtz was then dried at 110 °C and used in experiments at 5 and 10 kb. The results of these experiments show that amphibole does not persist above the solidus but that its breakdown defines the solidus. At 10 kb the solidus lies between 900 °C and 925 °C with Opx + Cpx + L above the solidus whereas, at 5 kb, the solidus is constrained between 900 °C and 950 °C with Anr + Opx + Cpx + L above the solidus.

In contrast to the H_2O-excess experiments, the dehydration melting experiments produced melts that are not corundum-normative but lie on the Anr–Opx tie-line on an ACM projection from quartz (Fig. 10). Thus, at lowered P_{H_2O}, the melts have shifted towards

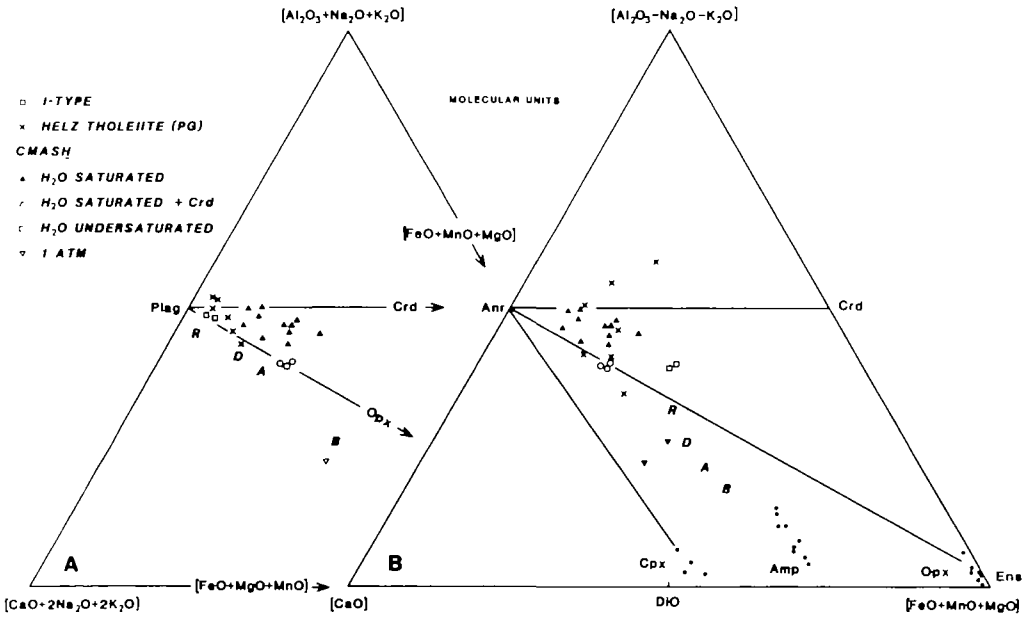

FIG. 10. A. An ACF-deluxe projection (O'Hara, 1976; Thompson, 1981) from SiO_2 and H_2O showing the compositions of melts and the ranges in mineral compositions (dots) obtained from the present CMASH experiments. The average chemical variation of the Cascades calc-alkaline rock series basalt-andesite-dacite-rhyolite (B–A–D–R) is replotted from Sekine *et al.* (1981, Fig. 3). The I-type granite minimum melts of White & Chappell (1977, table 1) are shown by squares. The liquid compositions obtained by Helz (1976, table 7a) for wet melting of Picture Gorge tholeiite at 5 kb P_{H_2O} from 700 °C to 1000 °C are shown by crosses. Symbols for CMASH melts; closed triangles—water saturated; open triangles—water saturated with Crd; open circles—dehydration melts; inverted triangles—1 atm melts. B. A conventional ACF projection from SiO_2 and H_2O of the data as shown in Fig. 10B. The removal of alkalis in this projection has the advantage of more clearly showing differences in peraluminous and metaluminous melt compositions but the disadvantage that feldspar-Qtz-H_2O minimum melts no longer plot at the Anr point.

being diopside-normative in character, but still not as strongly Dio-normative as in the 1 atm experiments. Relative to the Anr + Qtz (+ H_2O but without Dio) eutectic of Stewart (1967), these water undersaturated melts are also more Qtz-rich relative to water-saturated melts at the same P and T (Fig. 7). This is consistent with the compositional movement of the Qtz + Anr + H_2O eutectic as a function of P_{H_2O} (Fig. 7).

Thus, unlike the H_2O-excess experiments in which amphibole coexists with melt over a broad temperature interval above the solidus, the dehydration melting of amphibole defines the solidus in this system. Similar results are observed in the alkali- and iron-bearing systems investigated by Green (1973), in which the V-absent breakdown of amphibole defined the solidus for amphibole-bearing peridotite of pyrolite composition (pyrolite + 0·2 wt. per cent H_2O).

Even though the dehydration-melting reactions in Fig. 9A are not precisely located they still serve as a useful model for amphibolite melting over the pressure range appropriate to normal thicknesses of continental (35 km) and oceanic (15 km) crusts.

7.1 *Amphibolite melting in the model system CMASH*

An hypothetical set of metamorphic P–T paths are shown in Fig. 9A and denoted by the letters A through Q. The segment A to D is shown for simplicity to be isobaric. At B, Zoi + Tal + Qtz generate water-undersaturated melt with Anr + Amp, whereas at C, Zoi + Amp + Qtz generate a similar melt with Anr + Cpx. The amount of melt produced in either case depends upon the proportion of hydrous to anhydrous minerals.

Because of continuous reactions involving crystalline solutions (only $Al_2Mg_{-1}Si_{-1}$ (Amp, Cpx, Opx) and $CaMg_{-1}$ (Gar, Cpx, Opx) in CMASH) the amount of melt will slightly increase from C to D. Uplift is arbitrarily assumed to start at D on the P–T path. At E Amp undergoes dehydration-melting to produce an assemblage of anhydrous phases (varying proportions of Anr + Opx + Cpx + Qtz depending upon the initial amphibole) and a water-undersaturated melt. If this melt were tapped rapidly and moved quickly towards the surface along FGHI (for the choice of topology in Figs. 6 & 9), the melt would begin to resorb Cpx near H. This Cpx resorption would occur over a narrow P–T interval because of the existence of crystalline solutions. The melt would also boil within this temperature interval. Such a rock could contain vesicles and anhydrous minerals but no amphibole. Plagioclase would crystallize during ascent because of the experimentally documented movement of liquid away from Anr towards Qtz with decreasing pressure at constant temperature (see Figs. 2B & 7).

If similar melts produced at E were prevented from ascending at F or G, they would again crystallize amphibole at J or N respectively, and plagioclase would be resorbed. At successive reactions along the paths KLM or OPQ, the amount of water-undersaturated melt would decrease and release small amounts of water even though producing more amphibole. At M or Q respectively, the final melt would boil and, in both cases, would contain Amp in addition to anhydrous minerals. The crystallization interval of the deeper cooling path J to M is larger than the shallower path N to Q.

Such arguments also apply to the complex compositions of natural amphibolites not adequately represented by CMASH and emphasize the possibility that some volcanic rocks no longer containing amphibole may have been produced by melting of mafic crust (amphibolite without excess water) as may some plutonic suites containing amphibole.

The mineral–melt reactions depicted in Fig. 9 can also explain the common occurrence of corroded plagioclase with later euhedral plagioclase overgrowths in acid plutonic rocks and the scarcity of plagioclase resorption in chemically equivalent volcanic rocks. At temperatures above reaction (8) plagioclase would grow from the melt. Ascent from D to I would

cause continued precipitation of plagioclase and eruption of volcanic rocks with euhedral plagioclase and, depending upon ascent rate, little if any resorbed amphibole.

Amphibole-bearing mafic xenoliths incorporated in a magma at D would most likely be absent at shallow intrusion depths if the magma followed the ascent path E to H. The dehydration melting of the amphibole would probably result in the physical disintegration of such xenoliths. In contrast, amphibole in xenoliths in a magma which began ascent at temperature below D would not undergo dehydration melting and therefore would more likely be preserved during magma ascent.

A magma which cooled along the paths F–M or G–Q would first resorb early plagioclase, as this phase is on the high temperature side of the reactions (8) or (9). However, further plagioclase would crystallize just above the solidus (reaction 6) as well as at the solidus (reaction 5). Thus, resorbed feldspars could develop subsequent euhedral overgrowths. Melts that ascended and then cooled from temperatures lower than reaction (8) would not contain resorbed plagioclase.

8. SOME APPLICATIONS OF THE CMASH EXPERIMENTS TO AMPHIBOLITE MELTING AND RELATED MAGMA FRACTIONATION

As demonstrated here in CMASH and by Helz (1976) at 5 kb P_{H_2O} for hydrous natural basaltic compositions, the melts produced at the water-saturated solidus and up to at least 1000 °C are peraluminous. In contrast, melts formed by dehydration melting of amphibole-bearing assemblages in CMASH are only marginally metaluminous, lying on the Anr–Opx tie-line on an ACM projection from Qtz and H_2O (Fig. 10).

In Fig. 10 the basalt–andesite–dacite–rhyolite (BADR) trend of the Cascade lavas is plotted (Turner & Verhoogen, 1960, table 28). This differs from the Cascade trend shown by Sekine *et al.* (1981, fig. 3) in that the BADR compositions are replotted by adding alkalis in proportion to the aluminium in feldspar, and plotted in terms of the ACM-deluxe co-ordinates (see J. B. Thompson, 1981, p. 175; O'Hara, 1976, p. 110) projected from SiO_2 and H_2O. The BADR trend becomes only marginally metaluminous and certainly not peraluminous, as shown on plots where Na and K have not been compensated for (e.g. Sekine *et al.*, 1981). Also shown are White & Chappell's (1977, table 1) inferred initial I-type granite liquids; these are clearly metaluminous to peraluminous.

The peraluminous nature of the I-type minimum melts is similar to our experimental melts produced under water-saturated conditions, whereas the silicic variants of the BADR Cascades trend closely resemble our V-absent dehydration melts in their lack of obvious peraluminous (Cor-normative) or metaluminous (Dio-normative) character (Fig. 9). We consider the different feldspar/femics ratio in the natural rock samples compared to the CMASH experiments to simply reflect the absence of Na and K in our experiments. This would not change the peraluminous as opposed to metaluminous nature of different melts. The choice of co-ordinates in Fig. 10A permits a reasonable comparison of the melting studies in CMASH with natural rock compositions, because the alkalis in natural samples plot as alkali feldspar (at the same point as anorthite). Thus a model granite with feldspar + quartz + H_2O would plot at the Anr point; and biotite would plot at peraluminous compositions above the feldspar–Opx tie-line in Fig. 10A.

Melting of amphibolites at any depths under water-excess conditions could yield initially I-type 'granite' minimum liquids and at higher temperatures other members of the calc-alkaline suite. From the solidus to about 1000 °C these liquids are peraluminous; above that temperature they are metaluminous to peraluminous according to the results of Helz (1976). Such melts are clearly different from the BADR fractionation sequence which at B

(basalt) is clearly subaluminous (diopside-normative) and even at R (rhyolite) is only metaluminous, which could be accommodated by plagioclase plus aluminous Opx. It appears from Fig. 10, that the stabilization of the quartz–norite thermal divide (O'Hara, 1968) is important for some cases of BADR fractionation or even fractionation from andesite or dacite to rhyolite. This is especially true in view of the correspondence of the cross-over from corundum- to diopside-normative near 1000 °C for Helz's (1976) liquid compositions and the BADR fractionation trend.

Thus, if I-type 'granitic' rocks are genetically related to calc-alkaline volcanics, then an amphibolite source could not have been melted by dehydration melting reactions (in the absence of a fluid phase). The amphibolite sources must have been heated to temperatures well in excess of 1000 °C in order to attain a high proportion of melt from an andesitic or basaltic composition. The magma would then need to rise to shallow crustal levels and fractionate to the BADR trend where the norite divide became stabilized. Alternatively, the BADR trend could be either the product of melting at much lower P_{H_2O} and higher temperature at any crustal depth ($\leqslant$ about 10 kb) or the product of fractionation from a basaltic or andesitic parent magma with very low water content. Low-pressure fractionation of a basaltic parent would produce the BADR trend that is characterized by the presence of normative diopside.

Under circumstances of lower heat input to the base of the continental crust, I-type 'granites' produced at depth by melting of basaltic amphibolites would contain about 40 per cent melt (England & Thompson, 1985) while remaining peraluminous. Complete segregation may be expected with this proportion of melt to crystals and unmixing from restite is possible. However, plutonic crystallization at high P_{H_2O} would retain a peraluminous I-type character.

The classic calc-alkaline BADR fractionation trend of the Cascades, discussed above, is clearly not moving towards the peraluminous field. This could argue for the effect of the quartz–norite thermal divide in its evolution (either at high P_{H_2O} and very shallow depths, or at very low P_{H_2O} over greater depths). In contrast to the Cascades lavas, calc-alkaline volcanics from island arcs elsewhere in the world do contain peraluminous silicic members. As examples, glassy volcanic rocks from the Toba Tuffs ignimbrites of the Indonesian island arc (Beddoe-Stephens *et al.*, 1983) and also from the Tertiary Chihuahua province of New Mexico (Cameron & Hanson, 1982) are plotted in Fig. 11. In both cases the silicic lavas (rhyolites) are peraluminous. Hydrous phases are present in the Toba Tuffs ignimbrites whereas they are absent from many of the New Mexico lavas. Note that the melts are more peraluminous than phenocrystal biotite in the Toba Tuffs ignimbrites. Thus, in both areas the development of peraluminous silicic melts forming part of a BADR trend could have been due either to partial melting from an amphibolite source at high P_{H_2O} or else fractionation from a more mafic parent magma, again at high P_{H_2O}. The virtual absence of hydrous minerals in high water content rhyolitic ignimbrites from New Mexico is consistent with the petrographic predictions discussed earlier for an ascent path such as D–I in Fig. 9A, for which a hydrous lava may contain no hydrous minerals.

Isotopic and trace element techniques are required to distinguish between fractionation of primary basaltic material leading to calc-alkaline volcanics and melting of amphibolite to produce I-type granites (e.g. Cameron & Hanson, 1982); and between both of these and processes such as assimilation or magma mixing which could also produce strongly diopside-normative magma (J. D. Clemens, pers. comm., Jan. 1985). Certainly the proportion of 'granitic fraction' produced by melting of amphibolite is greater than that produced by fractionation.

The extent to which the original basalt composition (from nepheline- to quartz-normative)

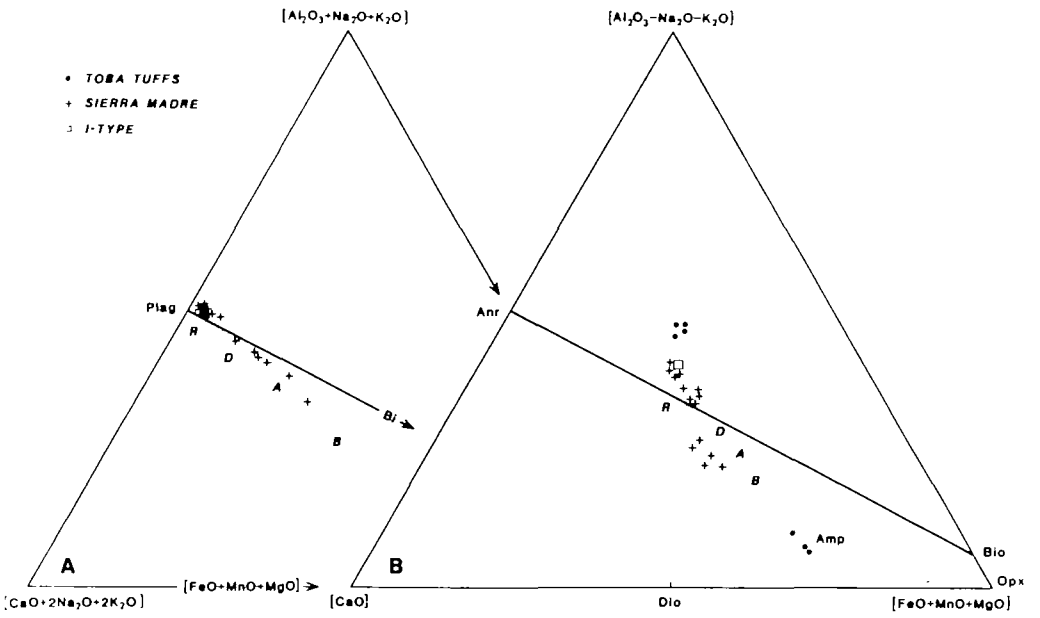

FIG. 11. A. An ACF-deluxe projection (ΣFe as FeO) from SiO_2 and H_2O showing the compositions of ignimbrites as well as melt inclusions within quartz and feldspar from the Toba Tuffs shown by dots (Beddoe-Stephens *et al.*, 1983) and the Sierra Madre Occidental, Mexican rhyolitic ignimbrites, basaltic andesite and dacitic lavas (Cameron & Hanson, 1982) shown by crosses. The compositions of White & Chappell's (1977, table 1) minimum I-type granite melt (open square) and the average BADR trend (shaded line) of Fig. 10 are also shown. Note that the peraluminous rhyolites are more aluminous than both the Bio–Plag and Opx–Plag tie-lines. Biotite, amphibole, and orthopyroxene mineral compositions are from the Toba Tuffs ignimbrites. B. A conventional ACF projection from SiO_2 and H_2O of the data shown in Fig. 11A.

is reflected in the presence of small amounts of different accessory minerals in amphibolites, may significantly influence the temperatures at which amphibolite melting may occur in oceanic or continental crust settings. The compositions of the partial melt fractions produced may also be affected.

As can be seen from Fig. 11, in Na- and K-bearing systems, biotite commonly takes the place of orthopyroxene. Thus, melting of plagioclase + biotite + quartz in natural compositions would also produce peraluminous melts incongruent to amphibole and clinopyroxene (Hoschek, 1976). As already pointed out for the Toba Tuffs, these melts are more aluminous than the Bio–Plag tie-line (Fig. 11).

9. THE EFFECT OF OTHER COMPONENTS ON AMPHIBOLE PHASE RELATIONS IN CMASH

Natural amphibolites contain essential Fe and Na as well as lesser amounts of other elements. The effect of these additional components on mineral stabilities may be investigated via phase relations in the model systems CFASH or NCMASH or by studying the subsolidus and melting behaviour of natural amphibolitic compositions.

9.1 *The relations of CFASH to CMASH*

According to Ernst (see summary diagrams in Gilbert *et al.*, 1982, p. 235), ferrotremolite breaks down to magnetite + fayalite + hedenbergite + quartz + H_2O some 400 °C below the Mg-tremolite breakdown at pressures to 3 kb. Similarly, grossular–almandine garnet will be

stable to much lower pressure in CFASH than garnets found in CMASH. Thus, the net effect of addition of FeO is to move the subsolidus dehydration reaction intersection with the solidus to higher pressure, expanding the subsolidus stability of garnet to lower pressures. The inevitable presence of Fe_2O_3 in iron-bearing systems would expand the stability of Zoi through pistacite substitution in epidote, of garnet through andradite substitution, of the amphiboles and pyroxenes, until eventual saturation with magnetite and/or hematite depending upon f_{O_2}.

9.2 *The relations of NCMASH to CMASH*

The addition of Na_2O to CMASH will result in continuous displacement of anorthite equilibria toward albite and the stabilization of 'hornblende' between tremolite and pargasite in composition. The effect on pyroxene chemistry will be small at low pressures but the jadeite component will be significant in pyroxene above 15–20 kb in quartz-bearing systems and at lower pressure in SiO_2-undersaturated compositions. The quartz-bearing system will not saturate with a common sodic phase, as happens in silica-undersaturated compositions in NCMASH through the appearance of nepheline.

The main effect of Na_2O is to stabilize Amp through $NaAlSi_{-1}$ exchange which is buffered by the presence of pairs of plagioclase + quartz + clinopyroxene (Thompson *et al.*, 1982). At low pressure the $NaSiCa_{-1}Al_{-1}$ exchange is minor in Amp + Cpx but major in Plg and L. Thus the relative importance of these two exchanges with sodium is difficult to predict.

In general, sodium will expand the stability of liquid more than amphibole more than plagioclase. Thus the solidus will be closer to Alb + Qtz + H_2O as evidenced by experimental water-saturated melting of basalt/amphibolite. Hornblende is subsilicic (certainly by comparison to tremolite). Thus, as with tschermakite, hornblende breakdown with quartz will occur at lower temperatures than at lower a_{SiO_2} (tremolite is an exception to this case). However, the net effect of adding $NaAlSi_{-1}$ to Amp and simultaneously $NaSiCa_{-1}Al_{-1}$ to plagioclase may result in hornblende + quartz stability being very close to the aluminous amphibole stability with quartz in CMASH. To extend the CMASH relation to NCMASH requires systematic study of hornblende + quartz + plagioclase + Opx.

10. CONCLUSIONS

1. In the pressure range of about 8 to 12 kb, dehydration-melting of Zoi + Tal + Qtz or Zoi + Amp + Qtz in model basaltic rocks to generate 'pseudogranitic' peraluminous liquids occurs only some tens of degrees above water-saturated melting of these assemblages. Talc is eliminated from further reaction just above 800 °C by its dehydration and zoisite is removed from basaltic compositions by the tie-lines among Cpx + Qtz + L + V. At pressures below 10 to 12 kb, water-saturated melting occurs slightly below that in Anr + Qtz + H_2O because MgO and excess Al_2O_3 are soluble in the melts. In this pressure range only Amp is available for dehydration melting and thus does not react in CMASH until 900–950 °C with the generation of water-undersaturated transitional metaluminous/peraluminous 'granitic' liquids.

2. The water-saturated melting reactions are controlled by the divides Anr + Opx, Anr + Tal, and Zoi + Tal (each with Qtz), with increasing pressure to 15 kb P_{H_2O}. In all cases the peraluminous liquids appear to be formed first in 'pseudopelitic' assemblages (containing the above tie-planes plus Crd, or Kya). Peraluminous liquids then occur at higher temperatures in model-mafic assemblages by the breaking of the thermal divides, permitting first Amp then Cpx to coexist with the liquids at successively higher temperatures. Quartz is lost from most mafic compositions through the formation of silicic liquids. By analogy with

hydrous melting of basalts (Helz, 1976, 1982), the melts remain corundum-normative to above 1000 °C, where it is expected that the continuous reaction in the assemblages Cpx + Amp + Qtz + L + V, or Cpx + Opx + Qtz + L + V causes them to become diopside-normative. The classical modal definition of peraluminosity obviously loses relevance when Anr is replaced by Zoi + Kya + Qtz etc., although they are still corundum-normative.

3. Melting of model amphibolites with excess water produces initial peraluminous melts at pressures above about 2 kb, which resemble I-type granites in their major element chemistry. A large range of calc-alkaline plutonic compositions can originate from amphibolite melting. Only by being heated to over 1000 °C can these melts become diopside-normative and would need to rise to shallow crustal levels (below about 5 km or 2 kb) to fractionate in a basalt–andesite–dacite–rhyolite (BADR) sequence of the Cascade type. The only slightly metaluminous character of the more fractionated magmas suggest that the quartz–norite divide may be active at low pressures where BADR fractionation occurs. This behaviour is likely to be enhanced when neglected components such as Na_2O, FeO, and Fe_2O_3 are added to the CMASH systems. This behaviour of thermal divides extends to where olivine and perhaps also spinel and nepheline are stable in low silica compositions, indicating similar peraluminous–metaluminous–subaluminous fractionation control in syenitic magma.

In contrast, dehydration (V-absent) melting in the crust is defined by the breakdown of amphibole (or biotite). Such melts are not obviously peraluminous in nature but are transitional between peraluminous and metaluminous. Some BADR suites (e.g. the Cascades) show a similar trend to the CMASH dehydration melts at high SiO_2 contents. If it could be demonstrated that such melts were not the products of magma mixing or assimilation, then these magma suites could be the result of either dehydration melting of amphibolite in the crust, low water-content fractionation from a recently mantle-derived basaltic or andesitic parent at any crustal depth, or high-P_{H_2O} fractionation at very shallow (< 5 kb) depths in the crust.

ACKNOWLEDGEMENTS

The project was commenced while D. J. Ellis was supported at E. T. H., Zurich by the Schweizerische Nationalfonds and completed at the University of Tasmania (where D. J. Ellis was a Queen Elizabeth II and A.R.G.S. Research Fellow).

Rolf Schmid gave technical support with the Zurich piston-cylinder apparatus. We acknowledge discussions with our colleagues P. Koons, R. Schmid, R. Varne, E. Reid, and D. H. Green, and thank A. Barnicoat, J. D. Clemens, B. Harte, and D. Vielzeuf for commenting on the manuscript. We thank Virginia Byers and Mary MacDougall for typing the manuscript and June Pongratz for drafting the diagrams.

REFERENCES

Andersen, O., 1915. The system anorthite–forsterite–silica. *Am. J. Sci.* **39**, 407–54.

Beddoe-Stephens, B., Aspden, J. A., & Shepherd, T. J., 1983. Glass inclusions and melt compositions of the Toba Tuffs, Northern Sumatra. *Contr. Miner. Petrol.* **83**, 278–87.

Boettcher, A. L., 1970. The system CaO–Al_2O_3–SiO_2–H_2O at high pressures and temperatures. *J. Petrology*, **11**, 337–79.

Boyd, F. R., 1959. Hydrothermal investigations of amphiboles. In: Abelson, P. H. (ed.). *Researches in Geochemistry*. New York: John Wiley & Sons, 377–96.

Brown, G. C., & Fyfe, W. S., 1970. The production of granitic melts during ultrametamorphism. *Contr. Miner. Petrol.* **28**, 310–18.

Cameron, K. L., & Hanson, G. N., 1982. Rare earth element evidence concerning the origin of voluminous mid-Tertiary rhyolitic ignimbrites and related volcanic rocks, Sierra Madre Occidental, Chihuahua, Mexico. *Geochim. cosmochim. Acta*, **46**, 1489–503.

Cawthorn, R. G., & Brown, P. A., 1976. A model for the formation and crystallisation of corundum-normative calc-alkaline magmas through amphibole fractionation. *J. Geol.* **84,** 467–76

—— & O'Hara, M. J., 1976. Amphibole fractionation and calc-alkaline magma genesis. *Am. J. Sci.* **276,** 309–29.

Chinner, G. A., & Schairer, J. F., 1962. The join $Ca_3Al_2Si_3O_{12}$-$Mg_3Al_2Si_3O_{12}$ and its bearing on the system CaO-MgO-Al_2O_3-SiO_2 at atmospheric pressure. *Ibid.* **260,** 611–34.

Delaney, J. M., & Helgeson, H. C., 1978. Calculation of the thermodynamic consequences of dehydration in subducting oceanic crust to 100 kb and > 800 °C. *Ibid.* **278,** 638–86.

Eggler, D. H., 1978. The effect of CO_2 upon partial melting of peridotite in the system Na_2O-CaO-Al_2O_3-MgO-SiO_2-CO_2 to 35 kb, with an analysis of melting in a peridotite-H_2O-CO_2 system *Am. J. Sci.* **278,** 305–43.

England, P. C., & Thompson, A. B., 1985. Thermal requirements for crustal melting in continental collision zones. *J. geol. Soc. Lond.* (in press).

Essene, E. J., Hensen, B. J., & Green, D H., 1970. Experimental study of amphibolite and eclogite stability *Phys. Earth planet. Interiors*, **3,** 378–84.

—— Wall, V. J., & Shettel, D., 1973. Equilibria in CaO-MgO-SiO_2-H_2O. *Trans. Am. geophys. Un.* **54,** 480.

Ford, C. E., 1976. Phase relations in the system CaO-MgO-Al_2O_3-SiO_2-H_2O. *Prog. expl. Petrol.* **3,** 266–72.

—— O'Hara, M. J., & Spencer, P. N., 1977. The origin of lunar feldspathic liquids. *Phil. Trans. R Soc. Lond.* **A285,** 193–7.

Gilbert, M. C., Helz, R. T., Popp, R. K., & Spear, F. S., 1982. Experimental studies of amphibole stability. In: Veblen, D. R., & Ribbe, P. H. (eds.) *Amphiboles: Petrology and experimental phase relations.* Miner. Soc. Am. *Rev. Mineralogy*, **9B,** 229–354.

Green, D. H., 1973. Experimental melting studies on a model upper mantle composition at high pressure under water-saturated and water-undersaturated conditions. *Earth planet. Sci. Lett* **19,** 37–53.

—— & Ringwood, A. E., 1967. An experimental investigation of the gabbro to eclogite transition and its petrological implications. *Geochim. cosmochim. Acta*, **31,** 767–833.

Gribble, C. D., & O'Hara, M. J., 1967. Interaction of basic magma with pelitic materials. *Nature*, **214,** 1198–201.

Griffin, B. J., 1979. *Energy dispersive analysis system calibration and operation with TAS-SUEDS, an advanced interactive data reduction package.* Dept. of Geology Publication, University of Tasmania, 44 pp.

Hansen, B., 1981. The transition from pyroxene granulite facies to garnet clinopyroxene granulite facies. Experiments in the system CaO-MgO-Al_2O_3-SiO_2. *Contr. Miner. Petrol.* **76,** 234–42.

Helz, R. T., 1976. Phase relations of basalts in their melting ranges at P_{H_2O} = 5 kb. Part II. Melt compositions. *J. Petrology*, **17,** 139–93.

—— 1982. Phase relations and compositions of amphiboles produced in studies of the melting behaviour of rocks. In: Veblen, D. R., & Ribbe, P. H. (eds.). *Amphiboles: Petrology and experimental phase relations.* Miner. Soc. Am. *Rev. Mineralogy*, **9B,** 279–346.

Hensen, B. J., 1976. The stability of pyrope-grossular garnet with excess silica. *Ibid.* **55,** 279–92.

Hoschek, G., 1976. Melting relations of biotite + plagioclase + quartz. *Neues. Jb. Miner. Abh.* 79–83.

Humphries, D J., Biggar, G. M., & O'Hara, M. J., 1972. Flow sheet for CaO-MgO-Al_2O_3-SiO_2 at atmospheric pressure. *Prog. expl. Petrol.* **2,** 138–9.

Jasmund, K., & Schäfer, R., 1972. Experimentelle Bestimmung der *P-T*-Stabilitätsbereiche in der Mischkristallreihe Tremolit-Tschermakit. *Contr. Miner. Petrol.* **34,** 101–15.

Jenkins, D. M., 1981. Experimental phase relations of hydrous peridotites modelled in the system H_2O-CaO-MgO-Al_2O_3-SiO_2. *Ibid.* **77,** 166–76.

—— 1983. Stability and composition relations of calcic amphiboles in ultramafic rocks. *Ibid.* **83,** 375–84.

—— Newton, R. C., & Goldsmith, J. R., 1983. Fe-free clinozoisite stability relative to zoisite. *Nature*, **304,** 622–3.

Johannes, W., Bell, P. M., Mao, H. H., Boettcher, A. L., Chipman, D. W., Hays, J. F., Newton, R. C., & Seifert, F., 1971. An interlaboratory comparison of piston-cylinder pressure calibration using the albite breakdown reaction. *Contr. Miner. Petrol.* **32,** 24–38.

Kushiro, I., 1972. Effect of H_2O on the composition of magmas formed at high pressures. *J. Petrology*, **13,** 311–44.

—— & Yoder, H. S., 1966. Anorthite-forsterite and anorthite-enstatite reactions and their bearing on the basalt-eclogite transformation. *J. Petrology*, **7,** 337–62.

—— —— 1972. Origin of calc-alkalic peraluminous andesite and dacite. *Yb. Carnegie Instn. Wash.* **71,** 411–13.

Newton, R. C., 1972. An experimental determination of the high-pressure stability limits of magnesian cordierite under wet and dry conditions. *J. Geol.* **80,** 398–420.

Nicholls, I. A., 1974. A direct fusion method of preparing silicate rock glasses for energy-dispersive electron microprobe analysis. *Chem. Geol.* **14,** 151–7.

Oba, T., 1978. Phase relationships of $Ca_2Mg_3Al_2Si_6O_{22}(OH)_2$-$Ca_2Mg_3Fe_2^{3+}Si_6Al_2O_{22}(OH)_2$ join at high temperature and high pressure—the stability of tschermakite. *J. Fac. Sci., Hokkaido Univ., Ser. IV,* **18,** 339–50.

Obata, M., & Thompson, A. B., 1981. Amphibole and chlorite in mafic and ultramafic rocks in the lower crust and upper mantle. *Contr. Miner. Petrol.* **77,** 74–81.

O'Hara, M. J., 1968. The bearing of phase equilibria studies in synthetic and natural systems on the origin and evolution of basic and ultrabasic rocks. *Earth Sci. Rev.* **4,** 69–133.

—— 1976. Data reduction and projection schemes for complex compositions. *Prog. expl. Petrol.* **3,** 103–26.

Osborn, E. F., & Muan, A., 1960. *Phase equilibrium diagrams of oxide systems.* Am. Ceram Soc.

Schairer, J. F., & Yoder, H. S., 1970. Critical planes and flow sheet for a portion of the system CaO-MgO-Al_2O_3-SiO_2 having petrological applications. *Yb Carnegie Instn. Wash.* **68,** 202–14.

Sekine, T., Wyllie, P. J., & Baker, D R., 1981. Phase relationships at 30 kbar for quartz eclogite composition in CaO-MgO-Al_2O_3-SiO_2-H_2O with implications for subduction zone magmas. *Am. Miner.* **66**, 938–50.

Stewart, D. B., 1967. Four-phase curve in the system $CaAl_2Si_2O_8$-SiO_2-H_2O between 1 and 10 kilobars. *Schweiz miner. petrogr. Mitt.* **47**, 35–59.

Thompson, J. B, 1981. An introduction to the mineralogy and petrology of biopyriboles. In: Veblen, D. R. (ed.). *Amphiboles and other hydrous pyriboles—Mineralogy.* Miner. Soc. Am. *Rev. Mineralogy*, **9A**, 141–88

—— Laird, J., & Thompson, A. B., 1982. Reactions in amphibolite, greenschist and blueschist. *J. Petrology*, **23**, 1–27.

Troll, G., & Gilbert, M. C., 1972. Fluorine-hydroxyl substitution in tremolite. *Am. Miner.* **57**, 1386–403.

Turner, F. J., & Verhoogen, J., 1960. *Igneous and Metamorphic Petrology.* New York: McGraw-Hill Book Company.

Vernon, R. H., 1976. *Metamorphic Processes.* London: Allen & Unwin.

Warner, R. D, 1975. New experimental data for the system CaO-MgO-SiO_2-H_2O and a synthesis of inferred phase relations. *Geochim. cosmochim Acta*, **39**, 1413–21.

White, A. J. R., & Chappell, B. W., 1977. Ultrametamorphism and granitoid genesis. *Tectonophysics.* **43**, 7–22.

Wones, D. R., & Dodge, F. C. W., 1977. The stability of phogopite in the presence of quartz and diopside. In: Fraser, D. G. (ed.). *Thermodynamics in Geology.* Dordrecht: Reidel, 229–47.

Wood, B. J., & Holloway, J. R., 1984. A thermodynamic model for subsolidus equilibria in the system CaO-MgO-Al_2O_3-SiO_2. *Geochim. cosmochim. Acta*, **48**, 159–76.

Yoder, H. S., 1965. Diopside-anorthite-water at five and ten kilobars and its bearing on explosive volcanism. *Yb. Carnegie Instn. Wash.* **64**, 82–9.

—— 1966. Spilites and serpentinites. *Ibid.* **65**, 269–79.

—— 1970. The join diopside-pyrope-H_2O at 10 kb: its bearing on the melting of peridotite, the ACF metamorphic facies, and the gedrite-hornblende miscibility gap. *Ibid.* **69**, 176–81.